

**DEVELOPING OF LIPID-BASED NANOCARRIERS FOR
INCREASING GASTRO-INTESTINAL ABSORPTION
OF PLANT FLAVONOIDS**



**A Thesis Submitted in Partial Fulfillment of the Requirements for the
Degree of Doctor of Philosophy in Biomedical Sciences**

Suranaree University of Technology

Academic Year 2018

การพัฒนาตัวพาไขมันขนาดนาโนเพื่อเพิ่มการดูดซึมในกระเพาะอาหาร
และลำไส้ของสารฟลาโวนอยด์จากพืช




วิทยานิพนธ์นี้เป็นส่วนหนึ่งของการศึกษาตามหลักสูตรปริญญาวิทยาศาสตรดุษฎีบัณฑิต
สาขาวิชาชีวเวชศาสตร์
มหาวิทยาลัยเทคโนโลยีสุรนารี
ปีการศึกษา 2561

**DEVELOPING OF LIPID-BASED NANOCARRIERS FOR
INCREASING GASTRO-INTESTINAL ABSORPTION
OF PLANT FLAVONOIDS**


Suranaree University of Technology has approved this thesis submitted in partial fulfillment of the requirements for the Degree of Doctor of Philosophy.

Thesis Examining Committee



(Asst. Prof. Dr. Rungrudee Srisawat)

Chairperson



(Assoc. Prof. Dr. Nuannoi Chudapongse)

Member (Thesis Advisor)




(Asst. Prof. Dr. Piyada Ngernsoungnern)

Member




(Dr. Oratai Weeranantanapan)

Member




(Dr. Katawut Namdee)

Member



(Asst. Prof. Dr. Worawat Meevasana)



(Prof. Dr. Santi Maensiri)

Vice Rector for Academic Affair
and Internationalization

Dean of Institute of Science

จิตภา มุสิกะ : การพัฒนาตัวพาไขมันขนาดนาโนเพื่อเพิ่มการดูดซึมในกระเพาะอาหาร
และลำไส้ของสารฟลาโวนอยด์จากพืช (DEVELOPING OF LIPID-BASED
NANOCARRIERS FOR INCREASING GASTRO-INTESTINAL ABSORPTION OF
PLANT FLAVONOIDS). อาจารย์ที่ปรึกษา : รองศาสตราจารย์ ดร.นวลน้อย จุฑะพงษ์,
95 หน้า

เคอซิทินและลูปีนิ โพลินเป็นสารฟลาโวนอยด์จากพืช ซึ่งมีรายงานฤทธิ์ทางเภสัชวิทยาอยู่
หลายประการ สารทั้งสองมีแนวโน้มจะมีชีวปริมาณการออกฤทธิ์ต่ำเนื่องจากมีความสามารถในการ
ละลายน้ำได้น้อย วัตถุประสงค์หลักของการศึกษานี้คือการพัฒนาตัวพาไขมันขนาดนาโนเพื่อใช้
เป็นระบบนำส่งยาโดยมีเคอซิทินและลูปีนิ โพลิน (สกัดจากต้นชะเอมไทย) เป็นโมเดลต้นแบบ ตัว
พาไขมันขนาดนาโนที่ผลิตขึ้นแบ่งออกเป็น 3 ประเภท ได้แก่ solid lipid nanoparticles (SLN)
nanostructured lipid carriers (NLC) และ nanoemulsions (NE) ซึ่งถูกเตรียมด้วยเทคนิค
emulsification-sonification ตัวพาที่บรรจุเคอซิทินถูกผลิตขึ้นด้วยการเติมเกลือ น้ำดีที่มีความเข้มข้น
ตั้งแต่ 0.5 10 และ 15 มิลลิโมลาร์เข้าในส่วนผสม โดยสูตรที่ประสบความสำเร็จ คือ NLC ที่บรรจุ
เคอซิทิน (quercetin-loaded NLC; QNLC) ซึ่งมีส่วนประกอบของไขมันคือ glycerol monostearate
(GMS) และน้ำมันมะกอก ส่วนตัวพาลูปีนิ โพลินขนาดนาโนที่ผลิตได้ทั้ง 3 แบบ คือ LSLN LNLC
และ LNE นั้นมีคุณสมบัติเหมาะสมที่จะสามารถพัฒนาต่อเป็นระบบส่งยาที่ดีได้ โดยมี
ส่วนประกอบของไขมันคือ Dynasan[®] 116 และ/หรือ ไตรกลีเซอไรด์สายขนาดกลาง (MCT)

ได้ทำการตรวจสอบคุณสมบัติทางเคมีกายภาพและการปล่อยยาของตัวพาไขมันที่บรรจุ
ด้วยเคอซิทินและลูปีนิ โพลิน พบว่าองค์ประกอบที่เหมาะสมของ QNLCs คือการเติมเกลือ น้ำดีใน
ขนาดความเข้มข้น 5 มิลลิโมลาร์ โดยได้ขนาดอนุภาคในระดับนาโนที่ 115.5 ± 2.0 นาโนเมตร
มีการกระจายของขนาดอนุภาคแบบสม่ำเสมอ (ดูจากค่า PDI ที่เท่ากับ 0.200) และมีความเสถียรสูง
(เห็นได้จากค่าประจุที่ผิวอนุภาคที่เป็นลบ (-41.12 ± 0.38 มิลลิโวลต์) เคอซิทินถูกบรรจุลงในตัวพา
ขนาดนาโนด้วยเปอร์เซ็นต์การห่อหุ้มสูง (99.5%) และมีการบรรจุเคอซิทินในไขมันเท่ากับ 0.5%
เมื่อวัดการปล่อยเคอซิทินในสภาวะเลียนแบบทางเดินอาหาร พบว่าเคอซิทินถูกปล่อยออกมา 16.2%
ภายในเวลา 4 ชั่วโมง นอกจากนั้นผลการทดลองยังชี้ว่า QNLCs มีการปลดปล่อยยาอย่างช้าๆ ใน
ระบบหมุนเวียนเลือดแบบจำลอง ในกรณีของลูปีนิ โพลิน พบว่าตัวพาไขมันขนาดนาโนที่ดีที่สุดคือ
LNLC ซึ่งมีขนาดอนุภาค 151.5 ± 0.1 นาโนเมตร มีการกระจายของขนาดอนุภาคแบบสม่ำเสมอด้วย
PDI เท่ากับ 0.243 ค่าประจุที่ผิวอนุภาคเป็นลบที่ -41.18 ± 0.67 มิลลิโวลต์ มีเปอร์เซ็นต์การห่อหุ้มที่
99.3% และมีความสามารถในการบรรจุลูปีนิ โพลินในไขมันสูง (5.0%) และเมื่อเปรียบเทียบกับ

QNLCs พบว่า LNLC มีการปลดปล่อยลูปีนิโพลินออกมาในระบบหมุนเวียนเลือดแบบจำลองอย่างช้าๆ เช่นกัน แต่มีการปลดปล่อยสารออกมาในทางเดินอาหารต่ำกว่า คือเพียง 3.7%

ความสามารถในการซึมผ่านลำไส้ของตัวพานขนาดนาโน ได้รับการประเมินในแบบจำลองผนังลำไส้ที่ใช้เซลล์ร่วมกันสามชนิด คือ Caco-2, HT29 และ Raji B ผลการศึกษาการขนส่งยาข้ามผนังลำไส้เล็กจำลองชี้ให้เห็นว่า QNLC ที่ประกอบด้วยเกลือน้ำดีขนาด 5 มิลลิโมลาร์ เป็นสูตรที่เหมาะสมที่สุดในการนำส่งยาเนื่องจากพบว่าสามารถเพิ่มการดูดซึมเคอซีดินอย่างมีนัยสำคัญเมื่อเทียบกับเคอซีดินแบบดั้งเดิม ประสิทธิภาพในการดูดซึมเคอซีดินจากทางเดินอาหารที่เพิ่มขึ้นนี้ได้รับการยืนยันโดยการศึกษาการดูดซึมผ่านลำไส้เล็กที่แยกจากตัวของสัตว์ทดลอง อย่างไรก็ตาม ในกรณีของลูปีนิโพลิน เนื่องจากความไวในการตรวจวิเคราะห์ด้วยเครื่อง HPLC ร่วมกับข้อมูลความเป็นพิษต่อเซลล์ ทำให้ความเข้มข้นที่เหมาะสมของลูปีนิโพลินในการทดสอบต่ำเกินกว่าที่จะตรวจพบได้จากการทดสอบการส่งยาผ่านผนังลำไส้เล็กจำลองในหลอดทดลอง ดังนั้นการศึกษาโดยใช้รูปแบบการดูดซึมผ่านลำไส้เล็กของสัตว์ทดลองที่กลับเอาด้านในออกจึงมีความน่าเชื่อถือมากกว่า ผลจากการศึกษาแสดงให้เห็นว่า ลูปีนิโพลินถูกดูดซึมผ่านระบบส่งยา LNLC ได้มากกว่าลูปีนิโพลินแบบดั้งเดิมถึง 16 เท่า สรุปได้ว่าการศึกษานี้ประสบความสำเร็จในการผลิตตัวพาไขมันขนาดนาโนที่บรรจุด้วยเคอซีดินและลูปีนิโพลินเพื่อใช้เป็นระบบนำส่งยาในการเพิ่มปริมาณการดูดซึม โภชนเภสัชภัณฑ์ทั้งสองชนิดนี้จากระบบทางเดินอาหาร อย่างไรก็ตามยังมีความจำเป็นจะต้องทำการทดสอบในสัตว์ทดลองเพิ่มเติมเพื่อยืนยันผลจากการศึกษานี้

มหาวิทยาลัยเทคโนโลยีสุรนารี

สาขาวิชาปรีคลินิก

ปีการศึกษา 2561

ลายมือชื่อนักศึกษา _____

ลายมือชื่ออาจารย์ที่ปรึกษา _____



26.6

JIDAPA MUSIKA : DEVELOPING OF LIPID-BASED NANOCARRIERS
FOR INCREASING GASTRO-INTESTINAL ABSORPTION OF PLANT
FLAVONOIDS. THESIS ADVISOR : ASSOC. PROF. NUANNOI
CHUDAPONGSE, Ph.D. 95 PP.

QUERCETIN/ NANOSTRUCTURE LIPID CARRIER/ BILE SALT/ LUPINIFOLIN
/ ORAL BIOAVAILABILITY

Quercetin and lupinifolin, plant flavonoids, have been reported to possess various pharmacological effects. Both compounds are most likely to exert low oral bioavailability because of their poor water solubility. The objective of this study was to develop lipid nanocarriers as drug delivery systems by using quercetin and lupinifolin (extracted from *Albizia myriophylla* Benth.) as the models of choices. Three types of nanocarriers; solid lipid nanoparticles (SLN), nanostructured lipid carriers (NLC) and nanoemulsions (NE) were prepared by emulsification-sonification technique. Quercetin-loaded nanocarriers were merged with 0, 5, 10, and 15 mM bile salts. The successful formulation of quercetin was quercetin-loaded NLC (QNLC), of which lipid compositions were glycerol monostearate (GMS) and olive oil. All three types of nanocarriers loaded with lupinifolin, LSLN, LNLC, and LNE, were successfully synthesized, of which lipid component were Dynasan[®]116 and/or medium chain triglyceride (MCT).

Physicochemical characterizations along with releasing profile of QNLCs and lupinifolin-loaded lipid nanocarriers were investigated. The optimal composition of QNLCs, which added with 5 mM of bile salts, exhibited nanoscale-size of 115.5 ± 2.0 nm, monodispersity distribution (as shown by PDI value of 0.200) and high stability (as

indicated by zeta potential -41.12 ± 0.38 mV). Quercetin was loaded in the nanocarriers with high percentage of encapsulation (99.5%) and 0.5% loading capacity. The QNLCs released quercetin in gastro-intestinal condition up to 16.2% in 4 hours and they showed a sustained release in simulated circulatory system. In the case of lupinifolin, the best lipid nanocarriers was LNLC, which demonstrated the particle size of 151.5 ± 0.1 nm, monodispersity distribution with PDI of 0.243, negative surface charge at -41.18 ± 0.67 mV, high encapsulation (99.3%) and high loading capacity (5.0%). Compare to QNLCs, LNLC exhibited prolonged release in simulated circulatory system, but produced lower release in gastro-intestinal condition (3.7%).

Intestinal permeability of the nanocarriers was further evaluated in triple co-culture cell model (Caco-2, HT29 and Raji B cells). The results from the *in vitro* transepithelial transport study indicated that QNLC with 5 mM bile salt was the optimal formulation as it significantly increased the absorption, compared to native quercetin. This enhancement in GI absorption was confirmed by an *ex vivo* intestinal permeability study. However, due to the sensitivity of HPLC along with toxicity data, the suitable concentration of lupinifolin could not be detected in the *in vitro* transepithelial transport model. Thus an inverted small intestine model was more reliable. The results from the *ex vivo* study indicated that lupinifolin was absorbed through LNLC with 16 times higher than the native form. In conclusion, quercetin- and lupinifolin-loaded lipid nanocarriers were successfully formulated as delivery systems to enhance oral bioavailability of these nutraceutical compounds. However, further *in vivo* experiment is needed to validate the results from this study.

School of Preclinic

Academic Year 2018

Student's Signature _____ 

Advisor's Signature _____ 

ACKNOWLEDGEMENTS

I would like to gratefully thank my advisor, Assoc. Prof. Dr. Nuanoi Chudapongse for giving me an opportunity to do the research under her supervision. It is to express my deepest appreciation to my advisor for her advice and support so that I could attend international academic conferences and work in other professional laboratory. Also special thanks to Dr. Oratai Weeranantanapan for her kindly advice.

I wish to express my sincere thanks to Dr. Katawut Namdee and Dr. Teerapong Yata, the researchers from NANOTEC, NSTDA for the opportunity to join the national and professional laboratory in drug delivery system, which gave me the invaluable experience and enhanced my knowledge and skills.

I also very appreciate my thesis chairperson, Asst. Prof. Dr. Rungrudee Srisawat and committee members, Asst. Prof. Dr. Piyada Ngermsoungnern, Dr. Oratai Weeranantanapan, and Dr. Katawut Namdee for their comments and suggestions on my thesis.

I would like to thank Science Achievement Scholarship of Thailand and Suranaree University of Technology for financial supporting my graduate study.

Finally, I am deeply indebted to my family for their endless supports and encouragements. Very special thanks are to my friends and lab mates, who have provided a good time and precious experiences.

Jidapa Musika

CONTENTS

	Page
ABSTRACT IN THAI.....	I
ABSTRACT IN ENGLISH	III
ACKNOWLEDGEMENTS.....	V
CONTENTS.....	VI
LIST OF TABLES	X
LIST OF FIGURES	XI
LIST OF ABBREVIATIONS.....	XIII
CHAPTER	
I INTRODUCTION.....	1
1.1 Background/problem.....	1
1.2 Research objective.....	3
1.3 Research hypothesis	3
1.4 Scope and limitation of the study.....	3
II LITERATURE REVIEW	4
2.1 Plant flavonoids and their effects	4
2.1.1 Quercetin.....	4
2.1.2 Lupinifolin	6
2.2 Lipid-based formulation	7
2.2.1 Nanoemulsion	8

CONTENTS (Continued)

	Page
2.2.2 Solid lipid nanoparticle (SLN).....	9
2.2.3 Nanostructured lipid carrier (NLC)	9
2.2.4 Surfactant.....	12
2.3 Drug release measurement of lipid-based nanocarriers	12
2.3.1 Sample and separate methods.....	12
2.3.2 Dialysis-based methods	15
2.4 Transportation mechanism of lipid carriers in oral administration	18
2.5 Intestinal and colonic permeability model	22
III MATERIALS AND METHODS	24
3.1 Chemicals and instruments.....	24
3.2 Preparation of lipid nanocarriers	24
3.2.1 Fabrication of quercetin-loaded nanoemulsion (QNE).....	24
3.2.2 Fabrication of quercetin-loaded nanostructure lipid carrier (QNLC)...	25
3.2.3 Fabrication of quercetin-loaded solid lipid nanoparticles (QSLN)	26
3.2.4 Formulation of lupinifolin-loaded lipid nanocarriers	27
3.3 Physicochemical characterizations.....	28
3.3.1 Particle size and zeta potential.....	28
3.3.2 Encapsulation and loading capacity.....	29
3.3.3 Stability study	29
3.3.4 <i>In vitro</i> stability in gastro-intestinal (GI) tract condition.....	29
3.3.5 <i>In vitro</i> release in gastro-intestinal (GI) tract conditions.....	30

CONTENTS (Continued)

	Page
3.3.6 Drug releasing under PBS pH 7.4 condition	31
3.4 Intestinal and colonic permeability model	32
3.4.1 Cell culture.....	32
3.4.2 Cell viability assay: MTT assay	33
3.4.3 Transepithelial transport studies	33
3.5 <i>Ex vivo</i> intestinal permeability evaluation.....	34
3.6 HPLC analysis	35
3.6.1 Quercetin.....	35
3.6.2 Lupinifolin.....	36
3.7 Statistical analysis	36
IV RESULTS	37
4.1 Lipid nanocarriers of quercetin	37
4.1.1 Quercetin-loaded nanoemulsion (QNE)	37
4.1.2 Quercetin-loaded solid lipid nanoparticle (QSLN).....	40
4.1.3 Quercetin-loaded nanostructure lipid carrier (QNLC)	40
4.2 Characterization of lupinifolin-loaded lipid nanocarriers	47
4.2.1 Purification of lupinifolin	47
4.2.2 Size, PDI and zeta potential.....	50
4.2.3 Encapsulation efficiency (%EE), and loading capacity (%LC).....	50
4.2.4 <i>In vitro</i> stability in gastro-intestinal (GI) tract condition.....	53

CONTENTS (Continued)

	Page
4.2.5 Lupinifolin release in gastro-intestinal (GI) tract condition	54
4.2.6 Releasing profile	55
4.3 <i>In vitro</i> intestinal and colonic permeability model.....	56
4.3.1 Cell culture.....	56
4.3.2 Cell viability	57
4.3.3 <i>In vitro</i> transepithelial transport studies	59
4.4 <i>Ex vivo</i> intestinal absorption.....	61
4.4.1 Quercetin and its nanocarriers	61
4.4.2 Lupinifolin and its nanocarriers	61
V DISCUSSION AND CONCLUSION	64
REFERENCES	77
APPENDIX.....	91
CURRICULUM VITAE.....	95

LIST OF TABLES

Table	Page
2.1 The advantages and disadvantages of solid lipid nanoparticle (SLN)	10
3.1 The composition of quercetin-loaded lipid nanocarriers	26
3.2 The lipid component ratio of quercetin-loaded NLC (QNLC)	26
3.3 The composition of lupinifolin-loaded lipid nanocarriers	28
4.1 Size, PDI, and zeta potential of QNE	38
4.2 Size, PDI, zeta potential, encapsulation efficiency (%EE), and loading capacity (%LC) of QNLC.....	42
4.3 Comparison of ¹ H and ¹³ C NMR spectra of the yellow crystals extract from <i>A. myriophylla</i> in this study and lupinifolin	48
4.4 Size, PDI, zeta potential, encapsulation efficiency (%EE), and loading capacity (%LC) of lupinifolin nanocarriers.....	51
4.5 HPLC results of lupinifolin on <i>in vitro</i> intestinal absorption model	60
5.1 The characteristics of the best quercetin and lupinifolin-loaded nanocarriers	75

LIST OF FIGURES

Figure	Page
2.1 Structures of quercetin and its glucosides.....	5
2.2 Structure of lupinifolin.....	7
2.3 The characteristic composition of nanostructured lipid carriers (NLCs; A), solid lipid nanoparticles (SLNs; B) and nanoemulsions (NE; C).....	11
2.4 The schematic of syringe filter	13
2.5 A schematic of the centrifugal ultrafiltration with ultrafiltration tube	15
2.6 A schematic of dialysis bag method	16
2.7 A schematic of reverse dialysis.....	17
2.8 A schematic of Franz diffusion cell	18
2.9 Mechanisms of enhancing drug absorption of lipid-based nanocarriers	21
2.10 Intestinal and colonic permeability model.....	22
4.1 Quercetin-loaded nanoemulsions (QNE).....	38
4.2 Stability of QNE at room temperature.....	39
4.3 Quercetin-loaded solid lipid nanoparticles (QSLN)	40
4.4 Quercetin-loaded nanostructure lipid carrier (QNLC).....	42
4.5 Stability of QNLC at room temperature	43
4.6 Stability of quercetin nanocarriers	44
4.7 Quercetin release in gastro-intestinal tract condition.....	45
4.8 <i>In vitro</i> releasing profile of quercetin nanocarriers.....	46

LIST OF FIGURES (Continued)

Figure	Page
4.9 Lupinifolin crystals	47
4.10 Chemical structure of lupinifolin	49
4.11 Mass spectrum of lupinifolin purified from <i>A. myriophylla</i>	49
4.12 Lupinifolin-loaded lipid nanocarriers	51
4.13 Stability of lupinifolin nanocarriers at room temperature.....	52
4.14 Stability of lupinifolin nanocarriers in simulated GI condition	53
4.15 Lupinifolin release in gastro-intestinal tract condition	54
4.16 <i>In vitro</i> releasing profile of lupinifolin nanocarriers.....	55
4.17 The confluent Caco-2 cells	56
4.18 The effect of quercetin and QNLCs on cell viability of Caco-2 cells	58
4.19 The effect of lupinifolin and its nanocarriers on cell viability of Caco-2 cells ..	58
4.20 Quercetin intestinal absorption under triple co-culture <i>in vitro</i> cell model	59
4.21 <i>Ex vivo</i> intestinal absorption of quercetin	62
4.22 <i>Ex vivo</i> intestinal absorption of lupinifolin.....	63

LIST OF ABBREVIATIONS

DI	De-ionized
DLS	Dynamic light scattering
EMA	European Medicines Agency
EP	European Pharmacopoeia
FDA	Food and Drug Administration
HPLC	High performance liquid chromatography
JP	Japanese Pharmacopoeia
LNE	Lupinifolin-loaded nanoemulsion
LNLC	Lupinifolin-loaded nanostructure lipid carrier
LSLN	Lupinifolin-loaded solid lipid nanoparticle
MCT	Medium chain triglyceride
MTT	3-(4,5-dimethylthiazol-2-yl)-2,5-diphenyltetrazolium bromide
NE	Nanoemulsion
NLC	Nanostructure lipid carrier
PdI	Polydispersity index
QNE	Quercetin-loaded nanoemulsion
QNLC	Quercetin-loaded nanostructure lipid carrier
QSLN	Quercetin-loaded solid lipid nanoparticle
SGF	Simulated gastric fluid
SIF	Simulated intestinal fluid

LIST OF ABBREVIATIONS (Continued)

QSLN	Quercetin-loaded solid lipid nanoparticle
SGF	Simulated gastric fluid
SIF	Simulated intestinal fluid
SLN	Solid lipid nanoparticles
USP	United States Pharmacopoeia
ZP	Zeta potential



CHAPTER I

INTRODUCTION

1.1 Background/problem

Plant flavonoids are a large group of natural polyphenols that are almost extensively distributed in the plant kingdom. Flavonoids have been shown to have a wide range of biological and pharmacological activities in human health, for example, anti-allergic, anti-inflammatory, antioxidant, antimicrobial (antibacterial, antifungal, and antiviral), anti-cancer, and anti-diarrheal activities. There are multiple well-known flavonoids exerting several biological activities and have been considered as candidates for nutraceutical and pharmaceutical agents such as curcumin (Anitha et al., 2011; Dilnawaz and Sahoo, 2013; Kurien and Scofield, 2007; Mancuso, Siciliano, Barone, and Preziosi, 2012; Zhao, 2009), quercetin (Bilia, Isacchi, Righeschi, Guccione, and Bergonzi, 2014; Ghosh, Sarkar, Mandal, and Das, 2013; Priprem, Watanatorn, Sutthiparinyanont, Phachonpai, and Muchimapura, 2008; Sun et al., 2016), kaempferol (Chen et al., 2010; Khan et al., 2009), genistein (Zhao, 2009), and lupinifolin (Chansuwan, Palanuvej, and Ruangrunsi, 2016; Joycharat et al., 2013; Soonthornchareonnon, Ubonopas, Kaewsuwan, and Wuttiudomlert, 2004; Sutthivaiyakit et al., 2009; Yusook, Weeranantanapan, Hua, Kumkrai, and Chudapongse, 2017).

Quercetin (3,3',4',5,7-pentahydroxyflavone), a flavonoid found in various fruits and vegetables, tea, olive oil and red wine, has potential to be a nutraceutical and pharmaceutical agent (Priprem et al., 2008) because it has diverse pharmacology effects including anti-inflammatory, anti-allergy, antioxidant, anti-diabetic, anti-cancer, anti-anaphylaxis and anti-aging effects (Cai, Fang, Dou, Yu, and Zhai, 2013; Graefe et al., 2001; Mukhopadhyay and Prajapati, 2015; Sriraksa et al., 2012). Moreover, it has been shown to exhibit great potentials to ameliorate brain diseases such as, anti-Alzheimer, anti-brain cancer, anti-ischemia, and anti-Parkinsonism (Ghosh, Sarkar, Mandal, and Das, 2013; Maria, Ignacio, Marisol, Edison, and Gloria, 2016; Pan et al., 2015; Sriraksa et al., 2012; Zhang et al., 2016). However, the application of quercetin in pharmaceutical field is still limited due to its poor solubility, low bioavailability, poor permeability and instability.

Lupinifolin is a prenylated flavonoid isolated from several medicinal plants, such as *Myriopterion extensum* (Soonthornchareonnon et al., 2004), *Eriosema chinense* (Prasad, Laloo, Kumar, and Hemalatha, 2013; Sutthivaiyakit et al., 2009; Thongnest, Lhinhatrakool, Wetprasit, Sutthivaiyakit, and Sutthivaiyakit, 2013), *Albizia myriophylla* (Joycharat et al., 2013, 2016; Thammavong, 2013), and *Derris reticulata* (Chansuwan, Palanuvej, and Ruangrunsi, 2016; Kumkrai, Weeranantanapan, and Chudapongse, 2015; Mahidol, Prawat, Prachyawarakorn, and Ruchirawat, 2011; Prawat, Mahidol, and Ruchirawat, 2000; Yusook, Weeranantanapan, Hua, Kumkrai, and Chudapongse, 2017). There is evidence showing that lupinifolin possesses *in vitro* antimicrobial activities (Soonthornchareonnon et al., 2004; Sutthivaiyakit et al., 2009). However, due to its very insoluble property, poor oral bioavailability of lupinifolin is

anticipated (Yusook et al., 2017). Thus, lupinifolin as well as quercetin were used as the flavonoid candidates to improve oral bioavailability in this study.

In general, natural plant flavonoids enter to human body via ingestion. Oral administration is the convenient and cost-effective route for medication application due to less pain, high patient compliance, reduced risk of cross-infection, and needle stick injuries (Das and Chaudhury, 2011; Khan et al., 2015; O'Hare et al., 2013; Ou-Yang et al., 2013). However, various physiological barriers and first pass effects limit oral bioavailability. To improve the bioavailability after oral administration of quercetin and lupinifolin, numerous approaches have been undertaken, especially the potential lipid-based nanocarriers.

1.2 Research objective

To formulate and characterize lipid-based nanocarriers of two plant flavonoids (quercetin and lupinifolin) for improvement of their oral bioavailability.

1.3 Research hypothesis

The lipid-based nanocarriers loaded with quercetin and lupinifolin from this study are stable in condition of gastro-intestinal tract and circulation and during storage and enhance the *in vitro* and *ex vivo* absorption of native compounds.

1.4 Scope and limitation of the study

The bioavailability was investigated through *in vitro* and *ex vivo* drug release assay. Conformation of oral bioavailability of these products is necessary.

CHAPTER II

LITERATURE REVIEW

2.1 Plant flavonoids and their effects

2.1.1 Quercetin

Quercetin (3,3',4',5,7-pentahydroxyflavone), a plant flavonoid extracted from many fruits and vegetables, has been reported to exert various pharmacologic effects to human health (Graefe et al., 2001; Sriraksa et al., 2012). In plants, quercetin has been found mostly in leaves and other parts of the plants as aglycone and glycoside forms (Figure 2.1). The latter form is more abundant in nature. Quercetin glycosides, in which sugar groups are joined to phenolic groups by glycosidic bond, are changed to phenolic acids while they permeate the gastro-intestinal tract. Glucose, galactose and rhamnose are the most familiar sugars, which are usually found in flavonoid structure. In general, quercetin glycosides incorporate with a sugar group at the 3-position such as isoquercetin (quercetin-3-*O*- β -glucoside) or rutinoid quercetin (quercetin-3-*O*-rutinoside). A sugar group is typically conjugated to phenolic group at the 4'-position as quercetin 4'-*O*- β -glucoside and quercetin 3,4'-*O*- β -diglucoside. However, quercetin has not been approved as a therapeutic content by any regulatory agency and clinical studies.

Due to its neuroprotective potential by stimulating or inhibiting enzyme activities/signal transduction pathways (Ansaria, Abdula, Joshia, Opii, and Butterfielda, 2009; Sabogal-Guáqueta et al., 2015; Sriraksa et al., 2012; Yang et al.,

2016) and ability to penetrate to blood brain barrier (Ishisaka et al., 2011; Sriraksa et al., 2012), quercetin has been suggested to exert other beneficial effects on the central nervous system (CNS), such as anti-anxiety and cognitive enhancement. In addition, quercetin has been demonstrated to possess an anti-Alzheimer activity by decreasing extracellular β -amyloidosis, tauopathy, astrogliosis and microgliosis in the hippocampus and the amygdale (Ansaria et al., 2009; Zhang et al., 2016) .

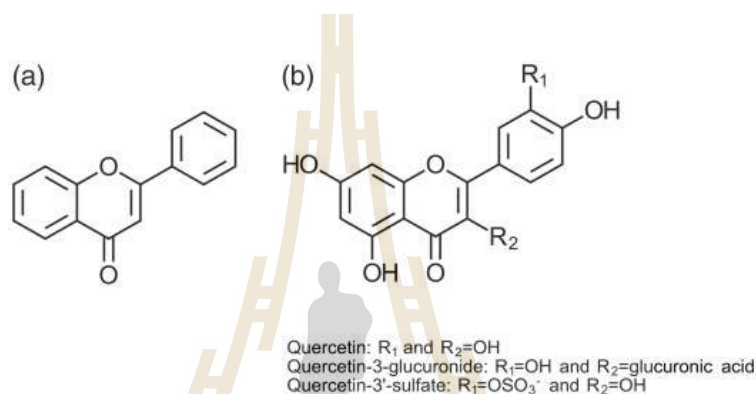


Figure 2.1 Structures of quercetin and its glucosides. (a) quercetin aglycone and (b) quercetin glycosides (McKay and Karamichos, 2017).

Nonetheless, several pharmacokinetic studies have shown that of quercetin has low oral bioavailability because of its poor absorption and rapid metabolism (Ferry, 1996; Graefe et al., 2001; Ou-Yang et al., 2013). Evaluated in ileostomy patients, 24% of total quercetin was absorbed following ingestion of 100 mg of the quercetin aglycone. Oral administration of 200 mg quercetin in 12 healthy people created the peak of plasma concentration only at 2.1 $\mu\text{g/ml}$. Its elimination half-life was about 11 hours (Graefe et al., 2001). Following single intragastric treatment of male Sprague-Dawley rats with 50 mg quercetin/kg body weight, free quercetin was found in the plasma only at a concentration of 0.27 $\mu\text{g/ml}$, and 93% of quercetin was metabolized

after one hour (Yang et al., 2016). To enhance the bioavailability and the drug targeting after oral absorption, techniques and modified materials of this agent are still necessary to be developed.

2.1.2 Lupinifolin

Lupinifolin ((8S)-5-hydroxy-8-(4-hydroxyphenyl)-2,2-dimethyl-10-(3-methylbut-2-enyl)-7,8-dihydropyrano[3,2-g]chromen-6-one), a prenylated flavonoid, has been reported to be a major compound in several plants (Chansuwan, Palanuvej, and Ruangrunsi, 2016; Joycharat et al., 2013, 2016; Mahidol, Prawat, Prachyawarakorn, and Ruchirawat, 2011; Prasad, Laloo, Kumar, and Hemalatha, 2013; Prawat, Mahidol, and Ruchirawat, 2000; Soonthornchareonnon, Ubonopas, Kaewsuwan, and Wuttiudomlert, 2004; Sutthivaiyakit et al., 2009; Thammavong, 2013; Thongnest, Lhinhatrakool, Wetprasit, Sutthivaiyakit, and Sutthivaiyakit, 2013). As shown in Figure 2.2, lupinifolin is a hydrophobic compound, which is insoluble in either acidic or neutral pH. The solubility of lupinifolin will be increased by strong alkalinity. However, in such condition, it will be degraded quickly like many flavonoids such as curcumin and quercetin (Kumavat et al., 2013; Schneider, Gordon, Edwards, and Luis, 2015). Furthermore, lupinifolin will be precipitated after diluting the stock solution in any organic solvent by water, which may cause the ambiguous results of various studies. Due to its very insoluble property, poor oral bioavailability of lupinifolin is anticipated. Techniques for material modification in nanoscale to enhance the oral bioavailability of plant flavonoids are valuable for drug delivery system development.

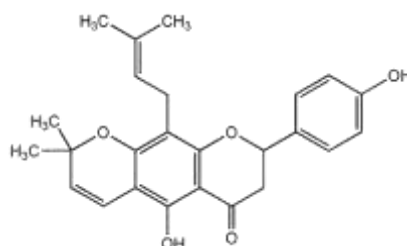


Figure 2.2 Structure of lupinifolin (Mahidol et al., 1998).

Lupinifolin has a wide range of pharmacological activities such as, anti-herpes simplex virus type 1, antimycobacterial, antidiarrheal, anticarcinogenesis and antioxidative activity (Prasad et al., 2013; Soonthornchareonnon et al., 2004; Sutthivaiyakit et al., 2009). Lupinifolin has shown several antimicrobial effects for example: anti-herpes simplex virus type 1 (Soonthornchareonnon et al., 2004), and antimycobacterial (Soonthornchareonnon et al., 2004; Sutthivaiyakit et al., 2009). It also exhibited a potent bactericidal effect against *Staphylococcus aureus* by disruption of bacterial cytoplasmic membrane (Yusook, Weeranantanapan, Hua, Kumkrai, and Chudapongse, 2017), supporting the antidiarrheal with a capable antibacterial activity (Prasad et al., 2013). A previous study reported a noticeable inhibitory effect in carcinogenesis test on mouse skin tumor stimulation (Itoigawa et al., 2002).

2.2 Lipid-based formulation

Colloidal drug carriers, such as micelles, nanosuspensions, polymeric nanoparticles, and liposomes are suggested to solve many poor oral absorption problems. Unfortunately, all of these carriers are not the potential drug delivery systems due to several difficulties; for example less stability, aggregation, drug releasing during storage, expensive large-scale production, organic solvent residues, cytotoxicity, etc.

Instead, the lipid-based nanocarriers are usually physiological lipids (biocompatible and biodegradable) which produce low acute and chronic toxicity (Chirio et al., 2014; Choi, Choe, Suh, and Ko, 2016; Hussein, Meihua, Fakurazi, and Ithnin, 2013). The Physicochemical diversity and biocompatibility of lipids and their ability to enhance oral bioavailability of drugs have made them as very potential carriers for oral drug delivery. Lipid nanoparticles are generally divided into three types: solid lipid nanoparticle (SLN), nanostructured lipid carrier (NLC) and nanoemulsion (NE).

2.2.1 Nanoemulsion

Nanoemulsion is the colloidal conducted from liquid lipid emulsified in water. This system exhibits several advantages for lipophilic drugs delivery, such as the use of biocompatible lipids, large-scale manufacturing, prevention of instable drugs from degradation, hydrolysis, and oxidation, enhancement of drug absorption, and controlled drug releasing (Aditya et al., 2014; Cai, Fang, Dou, Yu, and Zhai, 2013; Khan et al., 2015). However, nanoemulsions have numerous problems for example, restricted drug loading capacities, the expulsion of drug from the formulation, high surfactant concentration toxicity, and defeat of bioavailability enhancement due to drug precipitation on aqueous dilution *in vivo* situation (Khan et al., 2015).

The liquid lipid used in nanoemulsion should be a biodegradable, biocompatible, and consumable grade including natural plant oil (olive oil, soybean oil, palm oil, corn oil, coconut oil, sunflower oil, and groundnut oil), and essential oil (clover oil, lavender oil, rose oil, peppermint oil, tea tree oil, patchouli oil, and eucalyptus oil).

2.2.2 Solid lipid nanoparticle (SLN)

Lipid components of SLNs are solid form at room temperature and body temperature. SLNs usually are produced from a solid lipid or mixed with different solid lipids, such as cetyl palmitate, trimyristin (Dynasan[®]114), tripalmitin (Dynasan[®]116), tristearin (Dynasan[®]118), Glyceryl monostearate (geleol/Imwitor[®]900), Glyceryl palmitostearate (Precirol[®]ATO 5), Compritol[®]888 ATO (Aditya et al., 2014; Bahari and Hamishehkar, 2016; Das and Chaudhury, 2011; Rostami et al., 2014). There are several advantages and disadvantages of SLN formulations (Das and Chaudhury, 2011; Jawahar, Meyyanathan, Reddy, and Sood, 2012) as shown in Table 2.1.

2.2.3 Nanostructured lipid carrier (NLC)

The NLCs are solid lipids mixed with liquid lipids so that particle still is solid at room temperature and body temperature. Generally, drugs are blended between the fatty acid chains or in between lipid layers within SLN perfect crystalline grid. The formation of this perfect lipid crystalline structure leads to drug expulsion during storage (Das and Chaudhury, 2011) and low drug-loading proportion due to perfect crystal-transition of lipids (Oehlke, Behsnilian, Mayer-Miebach, Weidler, and Greiner, 2017). Therefore, NLCs have been developed to avoid these limitations. To decrease the drug expulsion of NLCs, drugs are mixed spatially in different lipid structure to create a lipid particle as imperfect as possible. Consequently, drug encapsulation and loading of NLC is greater and long-term colloidal is more stable than SLN and NE. The Figure 2.3 illustrates clearly the reason for higher drug payload of solid and liquid incompatible lipid matrix (NLCs; A) and lower drug and more expulsion in packed solid (SLNs; B) and lipid core oil (NE; C).

Table 2.1 The advantages and disadvantages of solid lipid nanoparticle (SLN)

Advantages	Disadvantages
Protecting the chemical-unstable drug from transformation during storage and in the stomach subsequently oral application	Drug encapsulation percentage less than other lipid-based carriers due to crystalline structure of solid lipid
Low cost of large scale production with uncomplicated technique	Possibility of aggregation and polymorphic transitions during storage
Biodegradable lipids with generally recognized as safe (GRAS) status	Drug expulsion after transition of lipid crystalline
Avoidance of organic solvents to fabricate SLN, minimizes the cytotoxicity	High water content of the dispersions (70-99.9%)
Decreasing photosensitive and moisture sensitive of drug.	Change of drug releasing profile during storage time

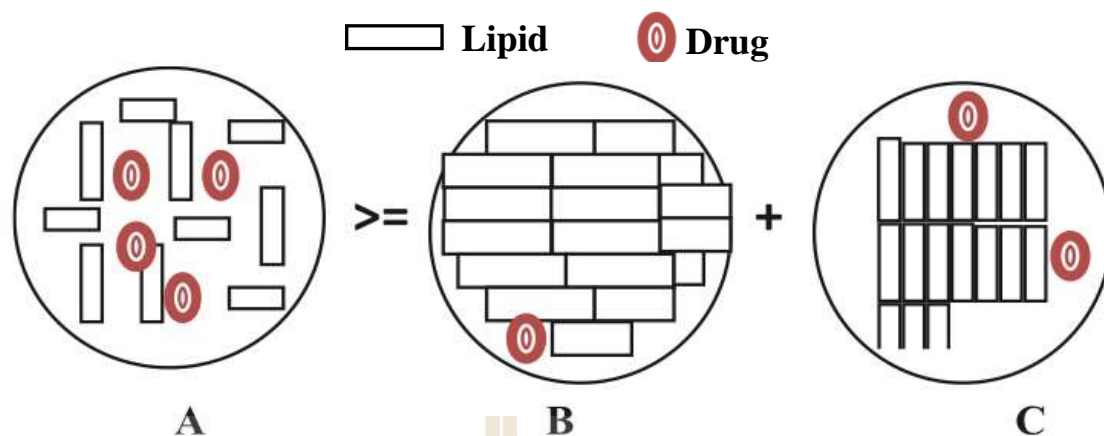


Figure 2.3 The characteristic composition of nanostructured lipid carriers (NLCs; A), solid lipid nanoparticles (SLNs; B) and nanoemulsions (NE; C). The picture is modified from illustration previously published by Khan and coworkers (2015).

Several liquid lipids, such as medium chain triglyceride (MCT; capric-caprylic and Miglyol), and various fruit or vegetable oil; olive oil, clove oil, lavender oil, palm oil, have been successfully used to construct NLC. The same solid lipids utilized in solid lipid nanoparticles have been typically used in NLC. The proportion between solid lipid and liquid lipid affects three different types of NLC, which are imperfect, multiple, and amorphous types. The imperfect type NLC executes the highest drug load by mixing more solid lipids than liquid lipids (oils). The multiple type NLC is the model which drugs are dissolved in oils and surrounded with solid lipid. Since crystallization or transformation of the solid lipid caused drug expulsion, the amorphous (shapeless) type NLC is produced by mixing special lipids like hydroxyl octacosanyl, hydroxyl stearate and isopropyl myristate to avoid solid lipid aggregation after cooling (Mukherjee, Ray, and Thakur, 2009).

2.2.4 Surfactant

Surfactants play an important role in some formulations of lipid nanoparticles. Adding enough surfactant and co-surfactant can prevent the aggregation and polymorphic transition of solid lipids. Moreover, the proportion and physical properties of surfactant could modulate the stability of nanocarriers (Salminen et al., 2014). Different surfactants are used for preparation lipid carriers such as phospholipids (soy lecithin, egg lecithin, and phosphatidylcholine), sorbitan ethylene oxide/propylene oxide copolymers (polysorbate 20, polysorbate 60, and polysorbate 80) and ethylene oxide/propylene oxide copolymers (poloxamer 188, poloxamer 182, poloxamer 407, and poloxamine 908).

2.3 Drug release measurement of lipid-based nanocarriers

The drug release testing method is important for the characterization of nanocarrier performance. Conducted under *in vitro* standardized conditions; it can provide the forecast of *in vivo* behavior of drug formulation. *In vitro* drug release testing methods for lipid-based nanocarriers are classified into: (1) sample and separate method and (2) dialysis-based methods. The details of each method are described below.

2.3.1 Sample and separate methods

A successful method to separate the lipid-based nanoparticles from the dispersal drug formulation is using a sample and separate method. This experiment is established in the release medium at stable temperature and samples are collected at precise time intervals. The fundamental of sample and separate procedure is the separation depending on the formulation properties. Most manner, centrifugation and filtration techniques, as well as solid phase extraction (SPE) procedures are utilized

(Zhang et al., 2014). To verify a complete separation, dynamic light scattering (DLS) and nanoparticle tracking analysis have been manipulated (Nothnagel and Wacker, 2018; Wallace et al., 2013). The principal of sample and separate procedure is the separation of drug and nanoparticles, which can be done by the following methods.

2.3.1.1 Filtration methods

A filter membrane is used to separate the dissolved drug content from colloidal nanoparticles. The majority drugs in nanocarriers express high lipophilicity, thereby the drug adsorption to different material needs consideration. Despite that, the scheme of the filtration method is uncomplicated, only basic apparatus and syringe filters (Figure 2.4) are accessible at low costs. The sampling procedure is similar to standardized release studies of macroscaled dosage forms.

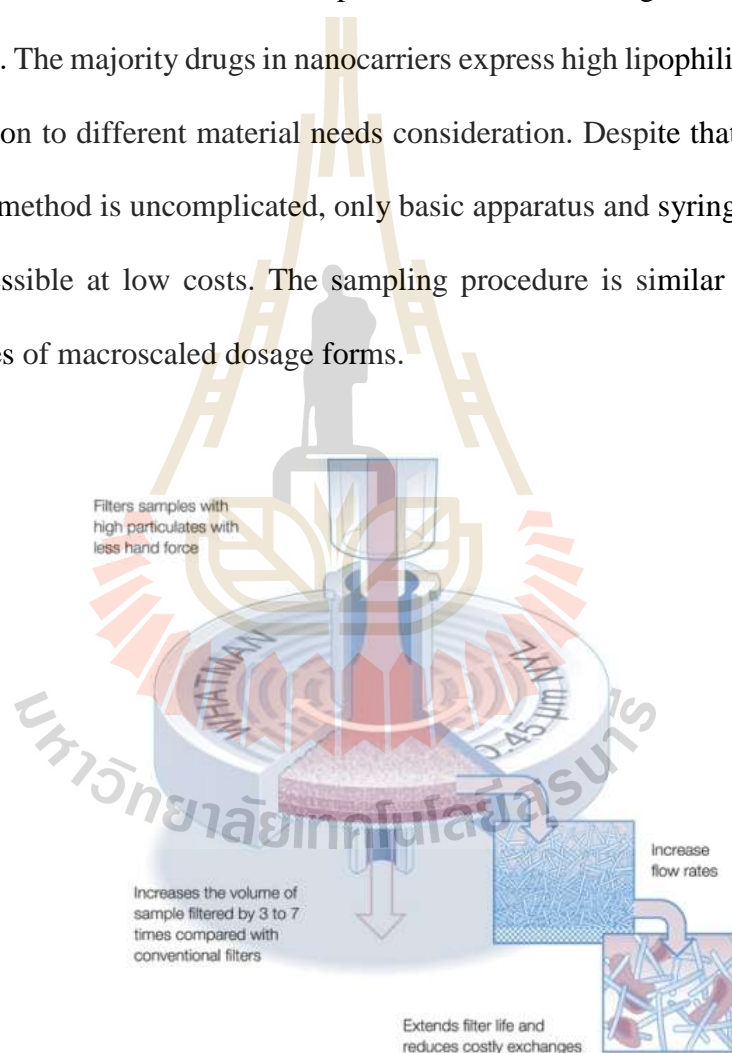


Figure 2.4 The schematic of syringe filter.

2.3.1.2 Preparative ultracentrifugation

Another procedure of separating the dissolved drug from the nanoparticle matter is the preparative ultracentrifugation. By the usage of high-speed centrifugation over a long interval of time, the particles of nanocarriers residue as a pellet in the sample tube. However, liposomes smaller than 100 nm could not be completely isolated in an ultracentrifugation process (Wallace et al., 2013). Low-density polymeric nanoparticles showed comparable effects of the lower nanometer range particles which have been denoted by the precipitation yields. A larger particle size perhaps reaches to the extended times of up to 20 hours during encapsulated drug is further released into the medium. Substance density, sampling viscosity, and particle size effected to the competence of this separation method (Wallace et al., 2013). Thus, the inquiry of quickly soluble formulations or slowly precipitating nanoparticles is not counseled. If drug release of larger particles is investigated, a centrifugation time should be shorter to complete separation of several nanosized formulations (Derakhshandeh, Hochhaus, and Dadashzadeh, 2011; Pacheco-Torres et al., 2015; Van Giau and An, 2016; Yücel and De, 2016; Yue et al., 2009).

2.3.1.3 Centrifugal ultrafiltration

Due to the precipitating of particles in the filter membrane, the efficiency of filtration is limited. Generally, the volume of medium passing through the membrane is increased while the particle size was decreased. Moreover, the composition of the release medium plays an important role. The solvent and emulsifier can extend the forces to the filter membrane. On the other side, centrifugal ultrafiltration via the ultrafiltration tube (Figure 2.5) empowers a gentle separation with reducing the formulation to high shear forces, so it is appropriate for the release study of sensitive

dosage forms. In the previous report, various separation of drugs from nanocarrier was constructed by filtrating it with the upper compartment membrane of the ultrafiltration unit (Yue et al., 2009). However, the sediments of particle and the liquid replacement in upper compartment have been taken in washing step. So this technique is unqualified for usual quality control.

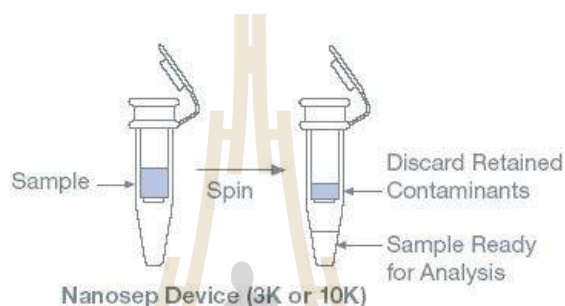


Figure 2.5 A schematic of the centrifugal ultrafiltration with ultrafiltration tube.

2.3.2 Dialysis-based methods

The free compound is separated from the colloidal with diffusion barriers of dialysis membranes. Equate to sample and separate methods, dialysis-based methods dispense separation of the released drug from nanoparticles. However, the procedure of data measurement is more complicate. At the start, the nanocarrier suspension is filled into the donor compartment, which is separated from the acceptor compartment by a dialysis membrane. The drug is fast transferred into the acceptor compartment through the dialysis method under optimized conditions. To evaluate the rate of drug transport, it should be handle as a routine experiment. The *in vitro* test should be processed under biomimic conditions to execute a valid prediction of *in vivo* release rates. The circulation inside the human body is established in phosphate buffer solution at pH 7.4.

2.3.2.1 Dialysis bag method

One of the desired techniques to study the drug releasing profile of nanocarriers is the utilization of the dialysis bag method. A dialysis bag with the filled sample performs as the donor compartment (Figure 2.6). The drug diffuses from the dialysis bag into the medium in acceptor compartment, which can be speed up with a shaker or stirrer to convince constant agitation. In this method, a separating effect can cause by charged particles and the viscosity impact of medium. However, a minimum volume ratio of 1:6 between the donor and the acceptor compartment is recommended (Souza, 2014).

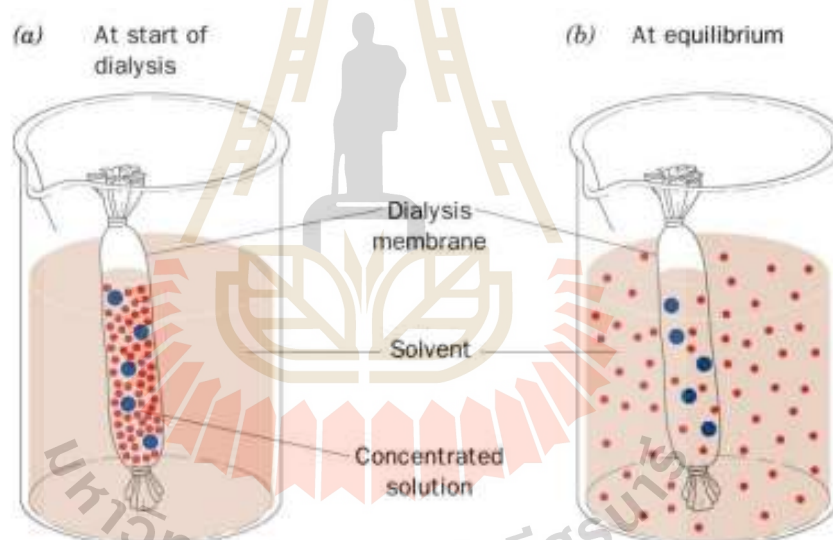


Figure 2.6 A schematic of dialysis bag method.

2.3.2.2 Reverse dialysis method

In reverse dialysis method, the acceptor compartment is inverted to the smaller compartment inside the dialysis bag, where samples are collected. A schematic of the apparatus is shown in Figure 2.7. The refined hydrodynamics and a high volume in the outer (donor) compartment are accountable for this issue. As a well-known

comprehension, reverse dialysis is prime of the dialysis bag technique. Anyway, the high sample dilution restricts the gradient between both compartments and as a consequence it limits the potential to separate drug from the formulations. Though, reverse dialysis is the least proper method for a physiological release study.

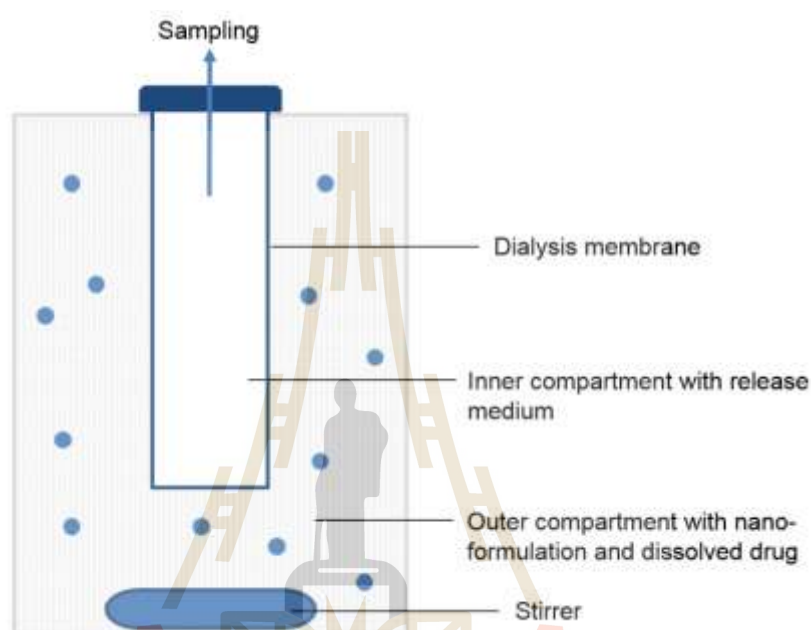


Figure 2.7 A schematic of reverse dialysis (Nothnagel and Wacker, 2018).

2.3.2.3 Franz diffusion cell

The Franz diffusion cell consists of two compartments separated by membrane layer. Nanocarriers are put in the upper compartment and the drug releases into the acceptor compartment (Figure 2.8). The temperature can be controlled to mimic physiological conditions of the skin and the immobility of water has improved by a magnetic stirrer in the acceptor compartment. The release profile depends on the stirring speed, membrane surface and thickness, temperature and sample volume. Membranes may comprise synthetic materials, cells or human and animal skin. Originally, the Franz diffusion cell was created for *in vitro* drug release studies for dermal and transdermal

applications (Yostawonkul et al., 2017). The physiological release condition is better illustrated by nanocarrier immobilization than by formulation suspension in release medium.

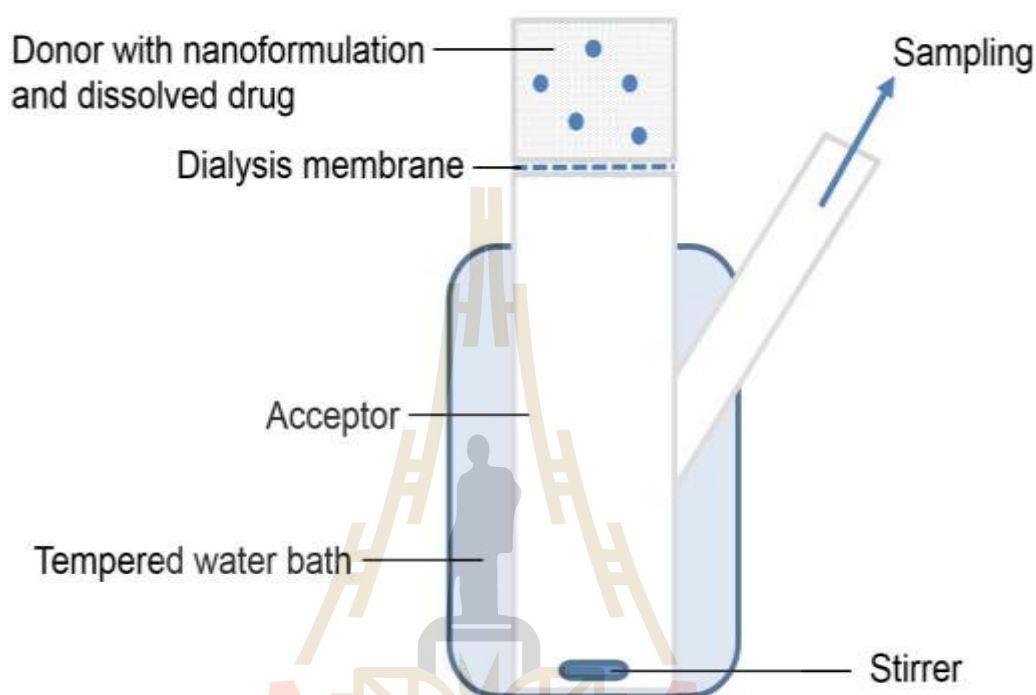


Figure 2.8 A schematic of Franz diffusion cell (Nothnagel and Wacker, 2018).

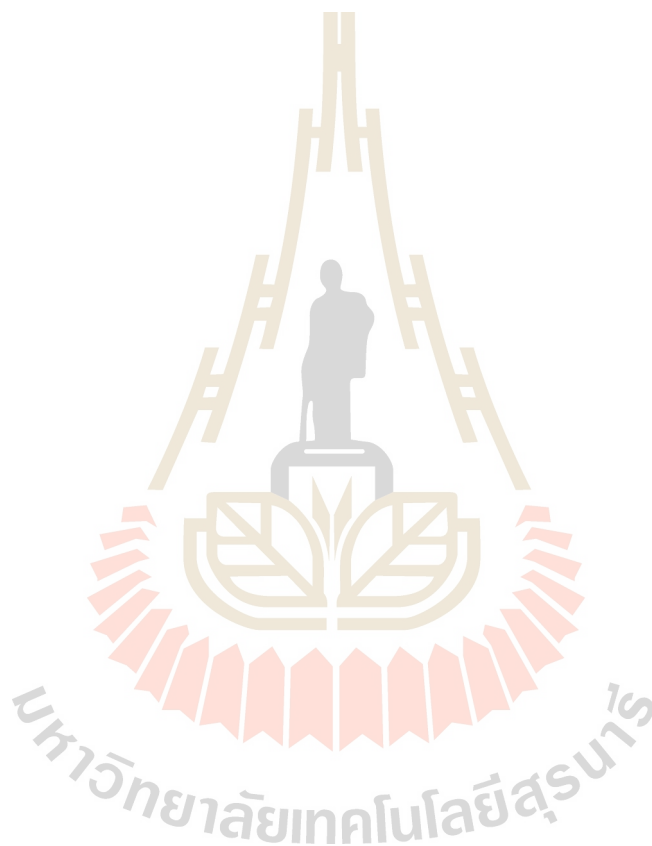
2.4 Transportation mechanism of lipid carriers in oral administration

After ingestion, lipid carriers can be absorbed into circulatory system by several pathways (Figure 2.9). For example, SLNs, NLCs, and other lipid vesicles can penetrate through tight junction, so called paracellular diffusion (Tan, Liu, Chang, Lim, and Chiu, 2012). SLNs can be transported through specialized microfold cells (M cells) of the Peyer's patches and other mucosa associated lymphoid tissues (MALT) by phagocytosis, receptor-mediated endocytosis and transcytosis into lymphatic systems (Jawahar et al., 2012; Mukhopadhyay and Prajapati, 2015). Another absorption is

mucoadhesion which the positive-charged nanocarriers can interact with negative-charged mucin (Choi et al., 2016; Y. Liu and Feng, 2015; Zhang, Tang, Xu, and Li, 2013). Liposome and other lipid carriers can permeate by endocytosis and macropinocytosis (the non-selective endocytosis). Nanoemulsions and the digested SLNs are absorbed by chylomicron-lymphatic absorption. This pathway initiates with the triglycerides in lipid carriers, which are digested into diglycerides and fatty acids with gastric lipases in stomach to exert the stable small sized lipid emulsion (micelles). These micelles are mixed with bile salts, cholesterol and phospholipids from gall bladder and pancreatic lipase/co-lipase from pancreas. The mixed micelles were absorbed by enterocytes along with acid pathway. These absorbed micelles are transformed to triacylglycerol in the enterocytes by re-esterified with monoacyl glycerol and then are combined with phospholipids and cholesterol ester to form a chylomicron. These chylomicron are released to lymphatic systems by exocytosis and then are secreted into the bloodstream (Bilia, Isacchi, Righeschi, Guccione, and Bergonzi, 2014).

Normally after drugs digestion and absorption into the enterocytes (transcellular absorption), drugs rapidly diffuse across the cell, and then are transported into the capillaries of portal vein. After metabolic processes in liver, the metabolized drugs are transmitted to the systemic circulation. However, some extremely lipophilic drugs (solubility in triglyceride > 50 mg/ml) can directly access to the systemic circulation by intestinal lymphatic route, which avoids hepatic first-pass metabolism. The potential candidates for lipid-based drug delivery are highly metabolized long-chain triglycerides. They are lipid core of intestinal lipoproteins formed in the enterocyte after re-esterification of free fatty acids and mono-glycerides and are absorbed through the

intestinal lymph. Short-chain triglycerides are primarily absorbed directly in the portal blood and drug can be transported through the lymphatic system. Therefore, to stimulate lipoprotein formation, compounds should compose of various lipids (mono-, di-, tri-glyceride, fatty acids, and phospholipids), which the mixed triglyceride (Miglyol), glycerol monostearate (GMS), and Dynadan[®]116 were used for the formulation in this study (Jawahar et al., 2012).



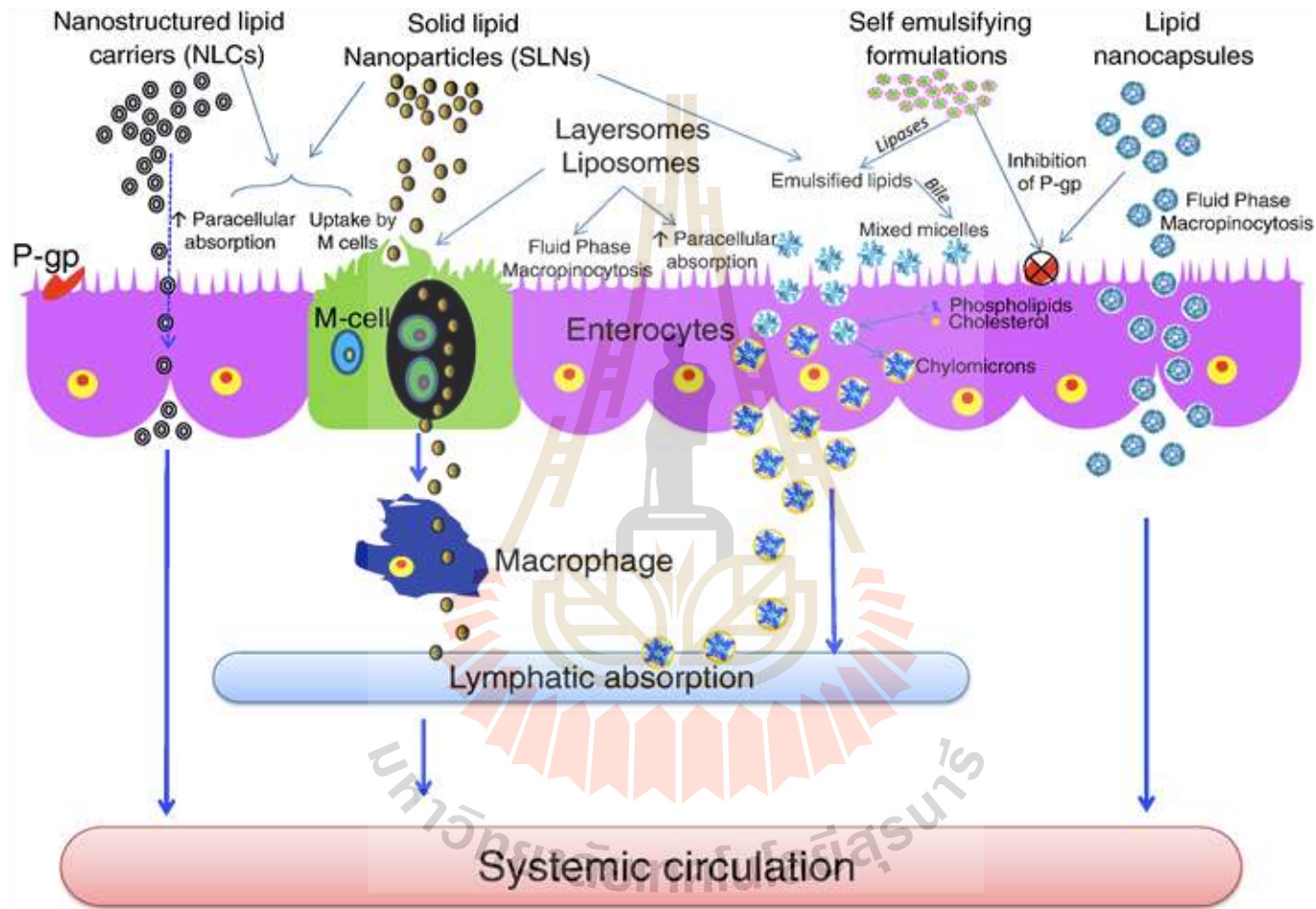


Figure 2.9 Mechanisms of enhancing drug absorption of lipid-based nanocarriers (Bilia et al., 2014).

2.5 Intestinal and colonic permeability model

The Caco-2 monolayer is an extensive accepted *in vitro* model to investigate human permeability (Derakhshandeh, Hochhaus, and Dadashzadeh, 2011; L. Liu et al., 2015; Picariello et al., 2013; Roche, Terres, Black, Gibney, and Kelleher, 2001). Caco-2 cells mimic similarly morphological and functional features to enterocytes. They express tight junctions, apical and basolateral sides, and well developed microvilli on the apical surface (Roche et al., 2001). However, Caco-2 monolayers have various limitations. They have less drug paracellular permeability because tight junctions are similar to colon epithelium cells and tighter than actually shown in the human small intestine. The human intestinal epithelium composes of absorptive cells (enterocytes), mucus producer cells (goblet cells), endocrine cells, and microfold cell (M cells), but Caco-2 cell model mimic only enterocytes and overexpress the efflux channel (P-glycoprotein).

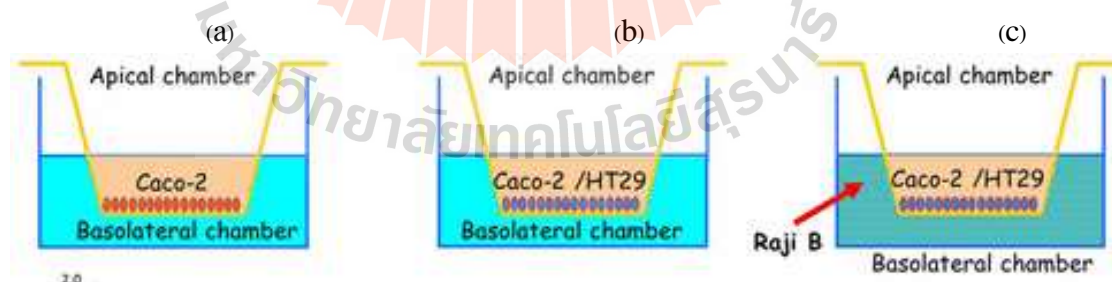


Figure 2.10 Intestinal and colonic permeability model. The Caco-2 monoculture model (a), intestinal and colonic Caco-2/HT29 (b) and Caco-2/HT29/Raji B (c) co-culture model (Lozoya-Agullo et al., 2017).

Hence, the alternative co-culture models are utilized to achieve more physiological function of the human intestinal epithelium (Figure 2.10) using the Caco-2/HT29 and the triple Caco-2/HT29/Raji B co-culture models (Lozoya-Agullo et al., 2017). In this study, the triple co-culture of Caco-2/HT29/Raji B model were operated to determine intestinal permeability and transport mechanism due to it is more physiological and complicated than Caco-2 monocultures.



CHAPTER III

MATERIALS AND METHODS

3.1 Chemicals and instruments

Clove oil, transcutool CG, poloxamer 188 (Pluronic F68), glycerol monostearate (GMS), glycerol, sodium cholate hydrate (bile salt), Tween 20, Span 80, pancreatin, and pepsin were purchased from Sigma-Aldrich (St. Louis, MO). Olive oil was purchased from Rafael Salgado (Spain). Quercetin hydrate was obtained from Sigma-Aldrich (Steinheim, Germany). Dynasan[®]116 was obtained from Sasol GmbH (Germany). Medium chain triglyceride (MCT) was purchased from Vicchi Enterprise (Thailand). De-ionized (DI) water was used throughout the study. Methanol, acetonitrile and acetic acid were HPLC grade. All other chemicals were analytical grade.

3.2 Preparation of lipid nanocarriers

3.2.1 Fabrication of quercetin-loaded nanoemulsion (QNE)

Nanoemulsions were prepared by low energy method through emulsification-sonification technique. Oil and water phase ratio was at 4:6 with surfactant and co-surfactant. An aqueous surfactant phase consisting of a hydrophilic surfactant Tween 20 and bile salt 0-15 mM were prepared and heated up to 65-70 °C before adding to the oil phase. Simultaneously, the lipid phase constituting lipophilic surfactant (lecithin and Span 80), clove oil, and quercetin were prepared and heated

up to 65-70 °C prior to addition of the water phase. Hot aqueous phase was dropped to lipid phase and simultaneously stirred at 2000 rpm for 2 minutes. The emulsion was ultrasonicated intermittently for 60s and cooled to room temperature. Blank NE was produced as the same method without an addition of quercetin to the formulation.

3.2.2 Fabrication of quercetin-loaded nanostructure lipid carrier (QNLC)

Nanostructure lipid carriers loaded with quercetin (QNLC) were prepared by emulsification-sonification technique. For each formulation, the ratio of oil phase and aqueous phase was used with the different volume of surfactant and cosurfactant (Table 3.2). The pre-warmed aqueous surfactant phase consisting of a hydrophilic surfactant (poloxamer 188, Tween 20, glycerol) and bile salt 0-15 mM were prepared and heated up to 65-70 °C before adding to the oil phase. Simultaneously, the lipid phase constituting lipophilic surfactant (Span 80) and quercetin along with the different lipid ratio solid lipid (GMS) and liquid lipid (clove oil, olive oil) were prepared and heated up to 65-70 °C prior to addition of the water phase. Hot aqueous phase was dropped to lipid phase and simultaneously stirred at 2000 rpm for 2 minutes. The emulsion was ultrasonicated intermittently for 60s and cooled to room temperature. The QNLCs were re-heated and repeated ultrasonication before cooling to room temperature. Blank QNLCs were produced as the same method without an addition of quercetin to the formulation.

Table 3.1 The composition of quercetin-loaded lipid nanocarriers.

Lipid phase	QNE	QNLC	QSLN
Solid lipid	-	0.2 g	1.0 g
Liquid lipid	1.0 g	0.8 g	-
Span 80	0.3 g	0.3 g	0.3 g
Quercetin	5 mg	5 mg	5 mg
Aqueous phase			
Poloxamer 188	0.3 g	0.3 g	0.3 g
Glycerol	2.1 g	2.1 g	2.1 g
Tween 20	0.2 g	0.2 g	0.2 g
DI	6.1 g	6.1 g	6.1 g
Bile salt 0, 5, 10, 15 mM			

Table 3.2 The lipid component ratio of quercetin-loaded NLC (QNLC).

Formulation	Lipid (%w/w)	Liquid lipid	Solid lipid : liquid lipid
QNLC1	15	Clove oil	4 : 1
QNLC2	10	Clove oil	4 : 1
QNLC3	10	Clove oil	1 : 4
QNLC4	10	Olive oil	1 : 4

3.2.3 Fabrication of quercetin-loaded solid lipid nanoparticles (QSLN)

Solid lipid nanoparticles loaded with quercetin (QSLNs) were prepared by emulsification-sonification technique. The lipid phase constituting lipophilic surfactant (Span 80) and quercetin along with solid lipid (GMS) were prepared at 65-70 °C.

Simultaneously, The pre-warmed aqueous surfactant phase consisting of hydrophilic surfactants (poloxamer 188, Tween 20, glycerol) and bile salt 0-15 mM were prepared at 65-70 °C prior to adding with hot aqueous phase and simultaneously magnetically stirred at 2000 rpm for 2 minutes. The emulsion was ultrasonicated intermittently for 60s at 65 °C and cooled to room temperature. Blank NLC were produced as the same method without adding quercetin to the formulation.

3.2.4 Formulation of lupinifolin-loaded lipid nanocarriers

3.2.4.1 Purification of lupinifolin

Lupinifolin was extracted from *A. myriophylla* Benth. Dried stems of *A. myriophylla* were extracted with the method modified from Yusook et al, 2017. Briefly, sixty grams of dried stem powder were extracted with 400 ml of hexane using a Soxhlet extractor. After 4-5 times washing with deionized water, the hexane extract was heated at 65 °C until it became clear. The hot clear hexane extract was left at room temperature overnight. The lupinifolin crystals were collected and kept in dried storage at room temperature. The characteristics of lupinifolin crystals were identified by nuclear magnetic resonance spectroscopy.

3.2.4.2 Synthesis of lupinifolin-loaded lipid nanocarriers

Three different types of lipid-based nanocarriers (SLN, NLC and NE) were produced using emulsification-sonification technique. An aqueous surfactant phase which consisted of distilled water and surfactant Tween 80 were heated up to 65-70 °C. Concurrently, the lipid phase constituting lipophilic surfactant (lecithin and Span 80), lupinifolin along with lipids of choice (SLN 100% (w/w) solid lipid (Dynasan[®]116), NE 100% (w/w) liquid lipid (Miglyol) and NLC mixture of solid and liquid lipids (20:80% w/w)] were prepared and heated up to 65-70 °C. Hot aqueous phase was added

to lipid phase and homogenized by magnetic stirrer at 2000 rpm for 2 minutes. The obtained emulsion was ultrasonicated intermittingly for 90s and cooled to room temperature. Blank nanocarriers were produced as the same method without adding of lupinifolin to the formulation. The compositions of the formulations are presented in Table 3.3.

Table 3.3 The composition of lupinifolin-loaded lipid nanocarriers.

Lipid phase	LNE	LNLC	LSLN
Dynasan [®] 116	-	0.2 g	1.0 g
MCT	1.0 g	0.8 g	-
Span 80	0.4 g	0.4 g	0.4 g
Lupinifolin	50 mg	50 mg	50 mg
Aqueous phase			
Poloxamer 188	0.4 g	0.4 g	0.4 g
Glycerol	2.0 g	2.0 g	2.0 g
Tween 20	0.2 g	0.2 g	0.2 g
DI	6.0 g	6.0 g	6.0 g

3.3 Physicochemical characterizations

3.3.1 Particle size and zeta potential

The samples were re-suspended in deionized water prior to measurements. The average size in diameter (nm), polydispersity index (PdI), and zeta potential (ZP) were

determined through dynamic light scattering (DLS) of Zetasizer, Nano-ZS (Malvern Instrument, UK). All measurements were performed at room temperature in triplicate.

3.3.2 Encapsulation and loading capacity

The total amount of quercetin and lupinifolin encapsulated and loading in lipid nanocarriers were determined by HPLC. First, the nanocarriers were centrifuged at 2000 rpm for 10 min at 4 °C. After centrifugation, free compounds are precipitated due to their water insoluble property. The supernatant (comprised of nanoparticles) was then discarded and free compound pellet was dissolved in ethanol prior to measurement. Amount of un-entrapped quercetin and lupinifolin were estimated with HPLC and calculated the indirect encapsulation efficiency and loading capacity using the following equations:

$$\text{Encapsulation Efficiency (\% EE)} = \frac{\text{Total compound} - \text{compound in pellet}}{\text{Total compound}} \times 100$$

$$\% \text{ Loading Capacity (\%LC)} = \frac{\text{Total compound} - \text{unencapsulated compound}}{\text{Total lipid}} \times 100$$

3.3.3 Stability study

The stability of fabrications were processed for 3 months. The samples were stored in the dim glass vials at 25 °C. After 1 and 3 months, the samples were characterized the size, ZP, and PDI.

3.3.4 *In vitro* stability in gastro-intestinal (GI) tract condition

3.3.4.1 Simulated stomach condition

To investigate the stability of lipid nanocarriers in gastro-intestinal (GI) tract condition, the particle sizes and PDI were conducted separately in simulated gastric fluid (SGF) and simulated intestinal fluid (SIF). This method was modified from the study

reported by Aditya and colleagues (2014). The intragastric stability of nanocarriers was detected in simulated gastric fluid (SGF). The samples (10 μ l) were suspended in 500 μ l of SGF (0.32% w/v pepsin, 0.2% w/v sodium chloride and pH adjusted to 2.0 ± 0.1 using 1 M HCl) and incubated in a water bath at 37 °C under shaking speed of 200 rpm. The samples were collected after 2 hours to analyze the size and PdI using the Zetasizer, Nano-ZS.

3.3.4.2 Simulated intestinal condition

The nanocarriers (10 μ l) were subjected to digestion in 500 μ l of simulated intestinal fluid (SIF), pancreatin 10 mg/ml in 50 mM KH_2PO_4 at pH 6.8 ± 0.1 , in a water bath at 37 °C under shaking speed of 200 rpm. After 2 h digestion in SIF, these samples were collected and centrifuged at 1500 g for 1 minute. to precipitate large mixtures (avoiding interferer). The supernatant was utilized to determine size and PdI of the digested nanocarriers using the Zetasizer, Nano-ZS.

3.3.5 *In vitro* release in gastro-intestinal (GI) tract conditions

3.3.5.1 Quercetin

To investigate the release from lipid nanocarriers in gastro-intestinal (GI) tract condition, the released quercetin and lupinifolin were examined in simulated gastric fluid (SGF) following by in simulated intestinal fluid (SIF). This method was modified from the study reported by Aditya and colleagues (2014). *In vitro* release in GI tract condition of quercetin nanocarriers were investigated using dialysis bag method. Dialysis membranes (pore size 3.5 kDa) were soaked overnight prior to experiment. Two ml of samples were added into the dialysis bags with 2 ml of SGF. The sample dialysis bags were put in 20 ml of the releasing media (10 mM phosphate buffer solution pH 7.4) and rotated at 200 rpm at 37 °C. After 2 h, 2 ml of sample in dialysis bag were

mixed with 2 ml of SIF and moved to new releasing medium. The 200 μ l of samples were collected and replaced with equal volume of releasing media at fixed time interval. The samples were kept at -80 °C until quantification using HPLC and the following equation:

$$\% \text{ Drug releasing} = \frac{\text{Drug in releasing media}}{\text{Total drug}} \times 100$$

3.3.5.2 Lupinifolin

In vitro release in GI condition of lupinifolin-loaded lipid nanocarriers were investigated using ultrafiltration with Amicon (50 kDa MWCO). Lipid nanocarriers (200 μ l) were mixed with 1.8 ml of SGF and incubated at 37 °C. After 2 h, the samples were collected and replaced with SIF 1 ml. The samples were collected after incubated at 37 °C for 2 h. Then, 1 ml of collected samples were mixed with 50% ethanol and centrifugation with Amicon at 5,000 g for 10 min. The samples were kept at -80 °C until quantification of lupinifolin content by HPLC.

3.3.6 Drug releasing under PBS pH 7.4 condition

3.3.6.1 Quercetin

The study of releasing under PBS (pH 7.4) condition of lipid nanocarriers was aim to mimic the release in blood circulation condition (Aditya et al., 2014). *In vitro* release of quercetin was investigated using dialysis bag method. Dialysis membranes (pore size 3.5 kDa) were soaked overnight prior to experiment. The known amount of sample was added into the dialysis bags with 4 ml of PBS pH 7.4. The sample dialysis bag was put in the sink media which composed of 30% ethanol in the releasing media

(10 mM PBS, pH 7.4) and rotated with 200 rpm speed at 37 °C. A sample (200 µl) was collected and replaced with equal volume of releasing medium at 30, 60, 120, 240, 360, 720, and 1,440 minutes. The samples were kept at -80 °C until quantification using HPLC.

3.3.6.2 Lupinifolin

The lupinifolin releasing was studied in PBS. One ml of each formulation was incubated with 9 ml of PBS pH 7.4 at 37 °C and 200 rpm rotation. The samples (1 ml) were collected at fixed time intervals and mixed with 50% ethanol. Lupinifolin contents after centrifugal-ultrafiltration with Amicon were measured with HPLC. Releasing profile was determined by comparing the amount of released lupinifolin with the total amount of loading capacity in lipid nanocarriers. Data were corrected taking in account of the dilution procedure.

3.4 Intestinal and colonic permeability model

3.4.1 Cell culture

The Caco-2, HT29, and Raji B cell lines were obtained from ATCC (Philadelphia, PA, USA). Dulbecco's Modified Eagle's Medium (DMEM) and Hank's Buffered Salt Solution (HBSS) was purchased from Gibco Life Technology. The Caco-2 cells were cultured in DMEM supplemented with 20% heat-inactivated fetal bovine serum (FBS), 1% L-glutamine, and penicillin/streptomycin (Gibco, Life Technology). HT29 was cultured in complete media (10% FBS in DMEM and penicillin/streptomycin). Raji B cells was cultured in α -MEM complete media (10% FBS and penicillin/streptomycin) and incubated at 37 °C in a humidified atmosphere containing 5% CO₂. Cells in log-phase growth were sub-cultured weekly by

trypsinization with 0.25% trypsin and were seeded at a ratio of 1:3 upon reaching 80% confluence. The culture media were changed every 2-3 days.

3.4.2 Cell viability assay: MTT assay

Caco-2 and HT29 cells at logarithmic growth phase were seeded into 96-well plates and incubated at 37 °C in an atmosphere of 5% CO₂ and constant moisture in the incubator. After the cells reach semi-confluence, the cultured cells were incubated with the native quercetin, quercetin-loaded nanoparticles (QSLN, QNLC and QNE), the native lupinifolin and lupinifolin-loaded lipid nanocarriers (LSLN, LNLC and LNE) in HBSS solution at the concentrations of 0-200 µg/ml and their equivalent amount (2 fold dilution) for 4 h. Then, HBSS solution was replaced by 100 µl of MTT solution (0.5 mg/ml), and the supernatant was discarded after 4 h of incubation at 37 °C. The cells were shaken with 100 µl of DMSO for 10 min, and the absorbances were read on the microplate reader at 570 nm. The cell viability was calculated.

3.4.3 Transepithelial transport studies

The Caco-2 and HT29 cells were seeded into the inserts of the 12-well Transwell plates at the density of 1.0×10^5 cells/well (Caco-2: HT29 ratio is 9:1). The culture medium was replaced every day in the first week, and then at daily intervals for the apical (AP) side and 2 days intervals for the basal (BL) side until the transport experiment were performed on Day 21 after seeding. The AP and BL sides contained 0.5 and 1.5 ml of culture medium, respectively. The Raji B cells (1.0×10^5 cells/well) were added in the basal compartment at Day 14. Then, the DMEM and α -MEM (1:1) were used as the culture medium in BL compartment. The integrity and viability of the cell monolayers were evaluated by measuring transepithelial electrical resistance (TEER) values between AP and BL sides with Millicell-ERS system. The cell inserts

were considered as qualified only if the resistance reached 150-200 Ω cm². The lucifer yellow solutions (50 mM) were incubated for 1 hour before and after the experiment in order to ensure the monolayer integrity. Only monolayers with % lucifer yellow rejection more than 95 were used in this experiment.

On day 21, the transport experiment was initiated by removal of the culture medium from AP and BL sides. The co-culture monolayers were rinsed twice with pre-warmed Hanks balanced salt solution (HBSS) and were incubated with the same solution at 37 °C for 10 min. The native quercetin and their nanoparticles (QSLN, QNLC and QNE) or the native lupinifolin and their lipid nanocarriers (LSLN, LNLC and LNE) were diluted to non-toxic concentration with an appropriate volume of HBSS. The test compounds were added to the AP (0.5 ml) while the receiving chamber (BL side) contained the corresponding volume of HBSS (1.5 ml). Incubation was performed at 37 °C for 180 min. At 60 and 180 min, each 200 μ l of the solution from BL was collected, and replaced with an equal volume of HBSS. The samples were frozen immediately and stored at -80 °C before analysis.

3.5 *Ex vivo* intestinal permeability evaluation

Female 8-week-old Wistar rats (body weight: 230 \pm 20 g) were obtained from the Laboratory Animal Center (SUT, Thailand). Animals were allowed ad libitum access to standard rat food and water. The animal procedure of this study was reviewed and approved by the Animal Research Care and Use Committee of Suranaree University of Technology, Thailand. All institutional and national rules for the care and utilization of laboratory animals were followed. The permeability evaluation method from the previous report was used with minor modification (Yen, Chen, Wu, Wang, and Wu,

2018). Briefly, each rat's entire small intestines were dissected and washed with normal saline (0.9%, w/v). The intestines were separated into three segments, duodenum, jejunum, and ileum, which were immediately placed in warm Tyrode's solution with oxygen. Each intestinal segment (length: approximately 4 cm) was inverted by a glass rod (diameter: 2 mm) and tied at one end. Subsequently, the opened sac was gently filled with Tyrode's solution and tied the other end. Then, the sacs were placed in flasks containing Tyrode's solution. The lupinifolin and quercetin with a final concentration of 50 $\mu\text{g/ml}$ as well as their nanocarriers were added into the flasks. After shaking at 37 °C for 1 h, each sac was cut open. The lupinifolin and quercetin contents were analyzed using HPLC method.

3.6 HPLC analysis

3.6.1 Quercetin

The quantitative analysis of quercetin was performed using an Agilent 1260 series chromatographic system (Agilent Technologies, USA) equipped with a pump, an autosampler and a diode array type of UV/VIS detector (DAD). Chromatographic separation was achieved by using a reverse-phase SB-C18 column (250 mm \times 4.6 mm, pore size 3.5 μm , Agilent Life Sciences). A mixture methanol and water (70:30 v/v) was used as mobile phase and adjusted pH to 3.64 with glacial acetic acid. The flow rate was 0.5 ml/min. The separation was performed with a detection at wavelength 374 nm, injection volume was 20 μl , and column temperature was 25 °C. Data were analyzed using an Agilent ChemStation Software.

3.6.2 Lupinifolin

The quantitative analysis of lupinifolin was performed using an Agilent 1290 series chromatographic system (Agilent Technologies, USA) equipped with binary pump, an autosampler and a diode array type of UV/VIS detector (DAD). Chromatographic separation was achieved by using a Poroshell 120, EC-C18 (4.6x50mm, pore size 2.7 μm , Agilent Life Sciences). A mixture acetonitrile and water (90:10 v/v) was used as mobile phase with flow rate 0.3 ml/min. The separation was performed with detection at wavelength 260 nm, injection volume was 10 μl , and column temperature was 25 $^{\circ}\text{C}$. Data were analyzed using an Agilent ChemStation Software.

3.7 Statistical analysis

Data were presented as mean and standard error of mean (mean \pm SEM) with n=3, except for some experiments that were specifically indicated in their figure legends. Statistical significance was analyzed by one-way or two-way ANOVA followed by the Student-Newman-Keuls test. Significant differences were indicated as * P <0.05.

CHAPTER IV

RESULTS

4.1 Lipid nanocarriers of quercetin

4.1.1 Quercetin-loaded nanoemulsion (QNE)

QNE was synthesized into 4 formulations with different bile salt concentrations, QNE-0, QNE-1, QNE-2, and QNE-3, which containing bile salts 0, 5, 10, and 15 mM, respectively. QNE-0 and QNE-1 appeared to be a milky yellowish dispersion, whereas QNE-2 and QNE-3 became transparent yellowish dispersion (Figure 4.1). The physicochemical properties of QNE are shown in Table 4.1. QNE formulations had various sizes (71.8-165.4 nm), polydispersity (PDI 0.29-0.58), and negative zeta potential. As shown in Figure 4.2A, the results from dynamic light scattering measurement showed that after 3 month-storage at room temperature, the average size of QNEs were 3-4 times larger (about 600 nm) than those of QNEs at day 1. Moreover, all formulations separated into two phases of solutions.

Table 4.1 Size, PdI, and zeta potential of QNE.

	Size (nm)	PdI	Zeta potential (mV)
QNE-0	165.4±12.3	0.418±0.008	-22.70±0.26
QNE-1	151.8.5±2.8	0.575±0.027	-24.97±0.37
QNE-2	94.9±4.9	0.444±0.006	-23.53±0.32
QNE-3	71.8±12.0	0.292±0.005	-21.30±0.17



Figure 4.1 Quercetin-loaded nanoemulsions (QNE). QNE-0: QNE without bile salt; QNE-1: QNE with 5 mM bile salt; QNE-2: QNE with 10 mM bile salt; QNE-3: QNE with 15 mM bile salt.

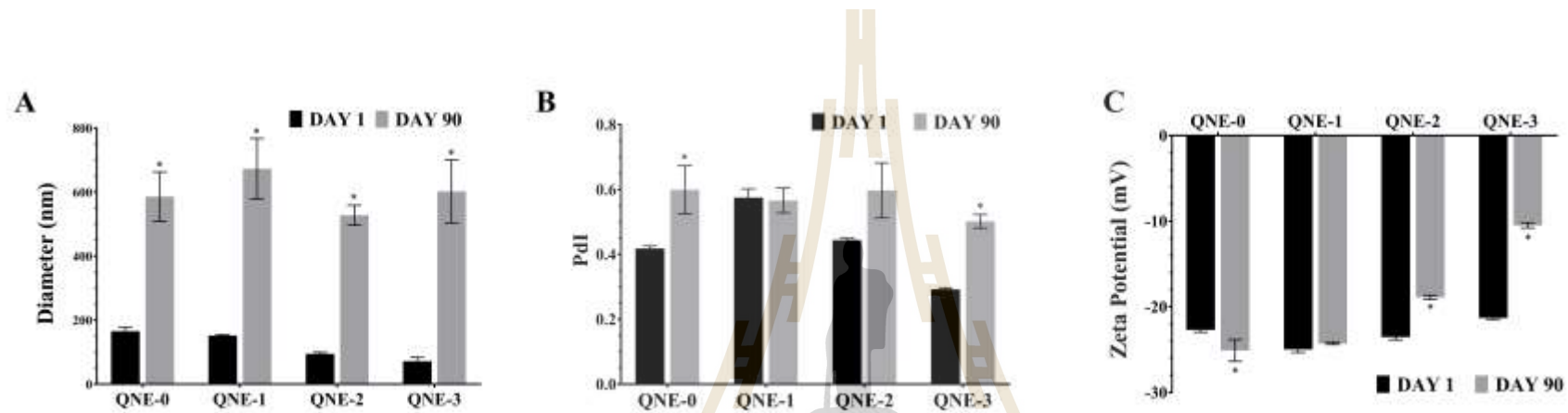


Figure 4.2 Stability of QNE at room temperature. Size (A), PDI (B), and zeta potential (C) of QNE after 3 months. QNE-0: QNE without bile salt; QNE-1: QNE with 5 mM bile salt; QNE-2: QNE with 10 mM bile salt; QNE-3: QNE with 15 mM bile salt; * $P < 0.05$, statistically significant difference compared to the first day of synthesis.

4.1.2 Quercetin-loaded solid lipid nanoparticle (QSLN)

QSLN was fabricated into 4 formulations with different bile salt concentrations, QSLN-0, QSLN-1, QSLN-2, and QSLN-3, which contained bile salts 0, 5, 10, and 15 mM, respectively. All QSLN products were successfully produced as milky yellowish cream (Figure 4.3). However, the physicochemical characterizations of QSLN could not be measured due to their instability and fast separation into two phases within 24 hours.



Figure 4.3 Quercetin-loaded solid lipid nanoparticles (QSLN).

4.1.3 Quercetin-loaded nanostructure lipid carrier (QNLC)

4.1.3.1 Size, PDI, and zeta potential

QNLC1, QNLC2, and QNLC3 showed instability and two-phase separation form within a week, thus their characterizations were not investigated. QNLC4 was successfully formulated as shown in Figure 4.4, which consisted of four products of nanostructure lipid carriers as light yellowish colloidal form (QNLC4-0, QNLC4-1,

QNLC4-2, and QNLC4-3). The formulations contained different concentrations of bile salts similar to QNE and QSLN. The average particle diameters of all QNLC4s were not significant different and in the range of 105 nm to 122 nm. The size distributions of the QNLC4 as determined by DLS exhibited miniature varied PDI (0.158-0.204), which indicated a narrow to moderate monodisperse population. The zeta potential (ZP) of the QNLC as a measurement for the surface charge was investigated to obtain more perception into the surface properties. The ZP of the QNLC in this study was in the range of -22 mV to -41 mV (Table 4.2). Blank NLCs displayed that the average size (109-120 nm), size distribution (PDI of 0.200), and zeta potential (-27 mV to -38 mV) were comparative to QNLC. The average size of all formulations increased about 5-15 nm during 3 months of storage. The results of DLS evaluation showed similar level of the size distribution and the surface charge with no significant difference (Figure 4.5).

4.1.3.2 Encapsulation efficiency (%EE), and loading capacity (%LC)

Encapsulation efficiency is the average proportion of encapsulated compound to total amount of the compound. All of the developed QNLCs showed prominent encapsulation up to 99% (Table 4.2). However, the drug loading capacity which refers to the amount of quercetin in the matter of nanoparticles in QNLC was only 0.5%.

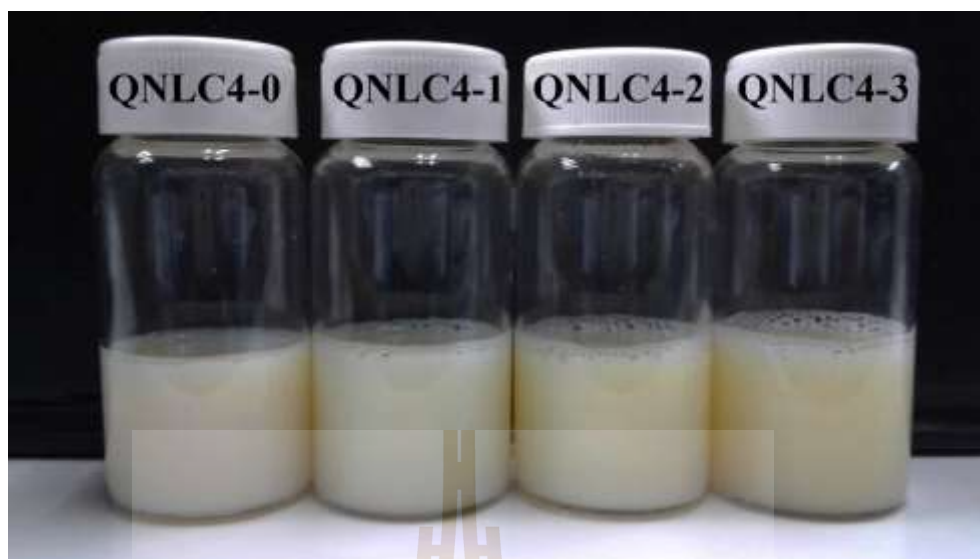


Figure 4.4 Quercetin-loaded nanostructure lipid carrier (QNLC).

Table 4.2 Size, PDI, zeta potential, encapsulation efficiency (%EE), and loading capacity (%LC) of QNLC.

	Size (nm)	PdI	Zeta potential (mV)	%EE	% DL
NLC4-0	120.4±1.8	0.232±0.023	-27.24±0.65	-	-
NLC4-1	118.5±2.3	0.214±0.050	-38.04±0.52	-	-
NLC4-2	113.1±2.1	0.249±0.018	-34.63±1.05	-	-
NLC4-3	109.2±1.9	0.204±0.012	-31.76±0.36	-	-
QNLC4-0	122.2±0.6	0.158±0.010	-22.31±0.53	99.5	0.5
QNLC4-1	115.5±2.0	0.200±0.011	-41.12±0.38	99.5	0.5
QNLC4-2	112.9±1.3	0.188±0.014	-33.39±0.31	99.6	0.5
QNLC4-3	104.6±2.4	0.204±0.014	-35.11±0.27	99.5	0.5

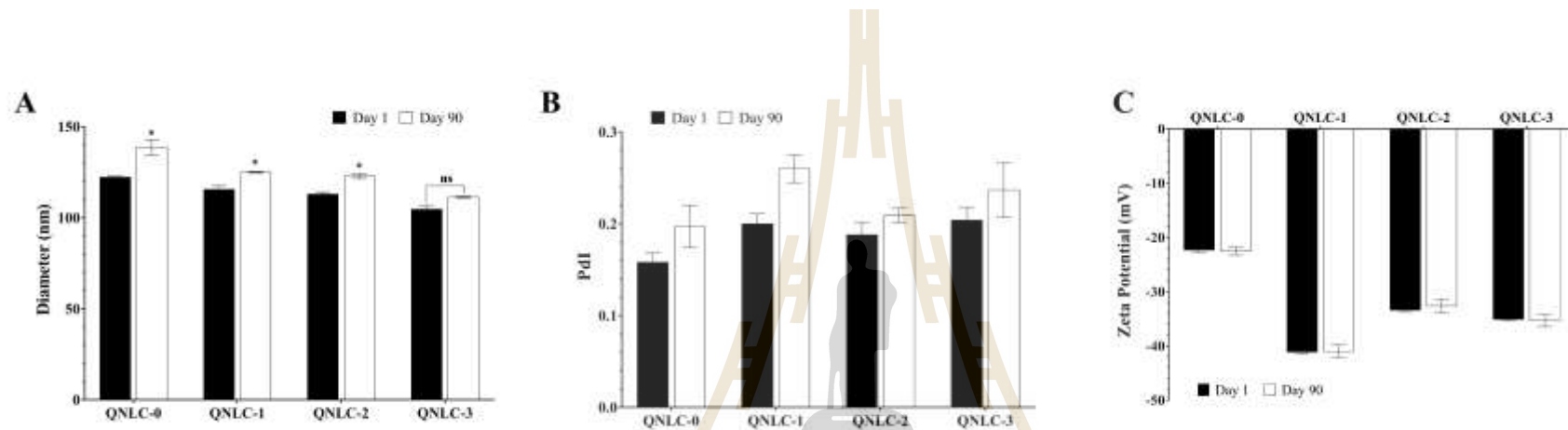


Figure 4.5 Stability of QNLC at room temperature. Size (A), PdI (B), and zeta potential (C) of QNLC after 3 months. QNLC-0: QNLC without bile salt; QNLC-1: QNLC with 5 mM bile salt; QNLC-2: QNLC with 10 mM bile salt; QNLC-3: QNLC with 15 mM bile salt; * $P < 0.05$, statistically significant difference compared to the first day of synthesis.

4.1.3.3 *In vitro* stability in gastro-intestinal (GI) tract condition

To investigate the effect of lipid composition on stability of nanocarriers, a simulated *in vitro* gastro-intestinal test was created in simulated gastric and intestinal fluids. The sizes of all QNLC formulations increased significantly during 2-hour digestion under simulated stomach (Figure 2A). In contrast, only the sizes of QNLC with bile salt significantly decreased under two-hour simulated intestinal digestion compared to the initial size (control) in PBS (Figure 2B).

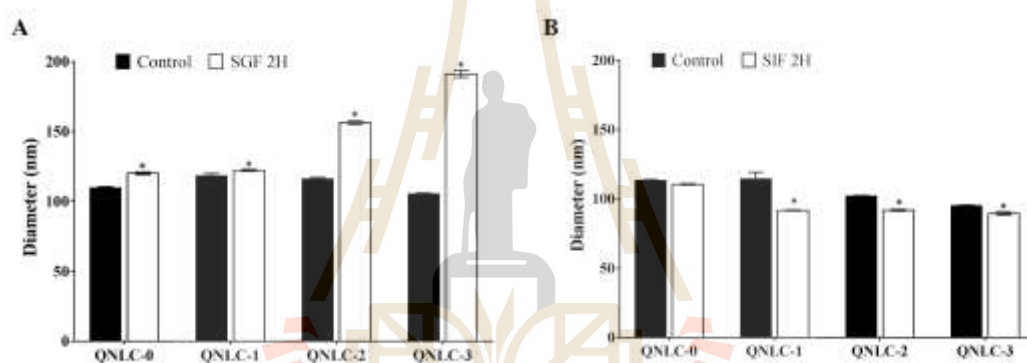


Figure 4.6 Stability of quercetin nanocarriers. Sizes of nanoparticles were measured in simulated stomach (A) and intestinal (B) conditions. QNLC-0: QNLC without bile salt; QNLC-1: QNLC with 5 mM bile salt; QNLC-2: QNLC with 10 mM bile salt; QNLC-3: QNLC with 15 mM bile salt; SGF: simulated gastric fluid; SIF: simulated intestinal fluid. Significantly difference at $*P < 0.05$, compared with control.

4.1.3.4 Quercetin release in gastro-intestinal (GI) tract condition

In vitro quercetin release was studied in simulated gastric-intestinal condition. QNLC formulations with low and high bile salts (QNLC-1 and QNLC-3, respectively), and QNLC formulation without bile salts (QNLC-0) were compared in this experiment. The release of quercetin from all types of nanocarriers was higher in SIF (about 16%) than SGF (about 7%). However, the different concentrations of bile salts showed no effect on the release of quercetin from nanocarriers in either SGF or SIF after 2-hour digestion (Figure 4.7).

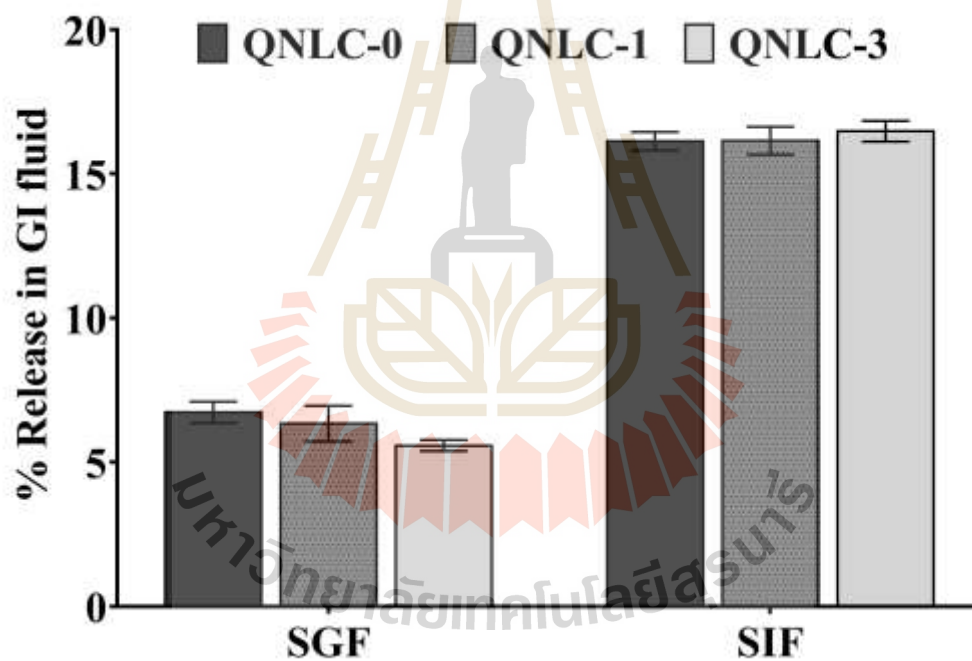


Figure 4.7 Quercetin release in gastro-intestinal tract condition. The experiment was tested in SGF and SIF for 2 hours. QNLC-0: QNLC without bile salt; QNLC-1: QNLC with 5 mM bile salt; QNLC-3: QNLC with 15 mM bile salt. ($P > 0.05$).

4.1.3.5 Releasing profile

The cumulative releasing profiles of QNLCs were determined by using a dialysis bag. The *in vitro* release of quercetin from the quercetin-loaded NLCs were approximately 4.33-5.23% at 24 hours (Figure 4.8). There was no significant difference in the quercetin release rate of QNLC-1 and QNLC-3, which compose of bile salt in the oil phase. In comparison, the quercetin release from QNLC-0 was less than those from QNLC-1 and QNLC-3.

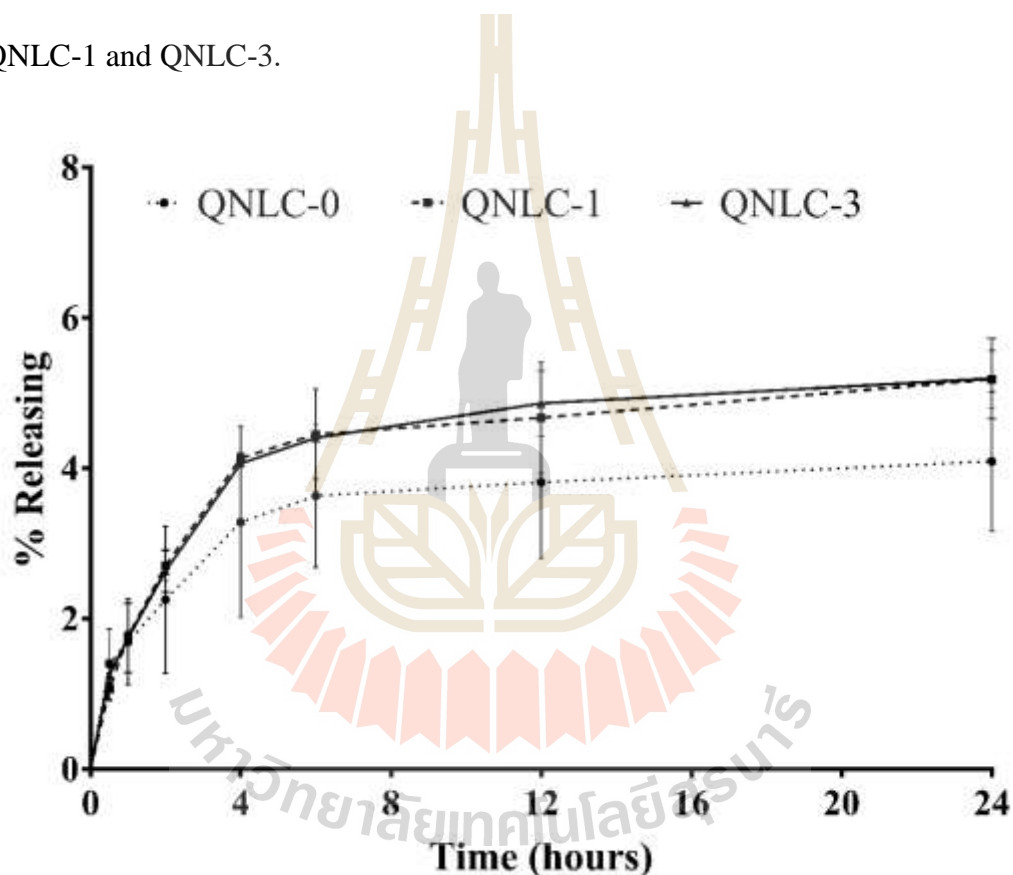


Figure 4.8 *In vitro* releasing profile of quercetin nanocarriers. The quercetin release was investigated under sink media. QNLC-0: QNLC without bile salt; QNLC-1: QNLC with 5 mM bile salt; QNLC-3: QNLC with 15 mM bile salt.

4.2 Characterization of lupinifolin-loaded lipid nanocarriers

4.2.1 Purification of lupinifolin

The lupinifolin, which was crystalized from the hexane extract, exhibited yellow needle-shaped crystal (Figure 4.9). The crystal yields about 2.5 mg of lupinifolin crystal/g of dried stem. The purity of lupinifolin was confirmed by the quantification of the ^1H and ^{13}C NMR spectroscopic as shown in appendix A (Mahidol et al., 1997). The spectra of lupinifolin, which purified from *A. myriophylla* stem, were consistent with the published data as shown in Table 4.3. Chemical structure of lupinifolin was illustrated in Figure 4.10. Its formula was confirmed by mass spectrometry. In the positive mode, $[\text{M}+\text{H}]^+$ at m/z 407.1859 (Figure 4.11) was consistent with the isotopic mass of lupinifolin (406.1780) which was previously reported. The purity of lupinifolin obtained from this study was more than 95% based on the NMR spectrum.



Figure 4.9 Lupinifolin crystals (40X magnification).

Table 4.3 Comparison of ^1H and ^{13}C NMR spectra of the yellow crystals extract from *A. myriophylla* in this study and lupinifolin.

Position	Yellow needle-shaped crystals ^a extract from <i>A. myriophylla</i> in this study		Lupinifolin ^b	
	δ_C (ppm)	δ_H (ppm)	δ_C (ppm)	δ_H (ppm)
2	78.52	5.32 (dd, 12.8, 2.8)	78.47	5.33 (dd, 12.6, 3.0)
3	43.23	3.04 (dd, 17.6, 12.8)	42.97	3.06 (dd, 17.1, 12.6)
β		2.78 (dd, 17.6, 3.0)		2.81 (dd, 17.1, 3.0)
4	196.48		196.84	
4a	102.66		102.61	
5	156.58		156.48	
6	102.83		102.79	
7	159.89		160.13	
8	108.63		108.73	
8a	159.36		159.44	
1'	131.05		130.60	
2'6'	127.71	7.33 (d, 8.4)	127.66	7.31 (d, 8.4)
3'5'	115.52	6.88 (d, 8.4)	115.53	6.89 (d, 8.4)
4'	155.87		156.09	
2''	78.14		78.20	
3''	125.99	5.51 (d, 10.0)	126.02	5.52 (d, 10.1)
4''	115.65	6.64 (d, 10.0)	115.53	6.64 (d, 10.1)
5''	28.30	1.43 (s)	28.25	1.45 (s)
6''	28.40	1.45 (s)	28.33	1.46 (s)
1'''	21.48	3.24 (d, 7.2)	21.42	3.22 (d, 7.2)
2'''	122.49	5.14 (dd, 7.2, 7.2)	122.40	5.16 (dd, 7.2, 7.2)
3'''	131.10		131.11	
4'''	17.83	1.65 (s)	17.78	1.66 (s)
5'''	25.82	1.65 (s)	25.74	1.66 (s)
5-OH		12.24 (s)		12.24 (s)

^a Reported of CDCl₃ at 500 MHz for ^1H -NMR and 125 MHz for ^{13}C -NMR

^b Reported of CDCl₃ at 300 MHz for ^1H -NMR and 75.6 MHz for ^{13}C -NMR (Mahidol et al., 1997)

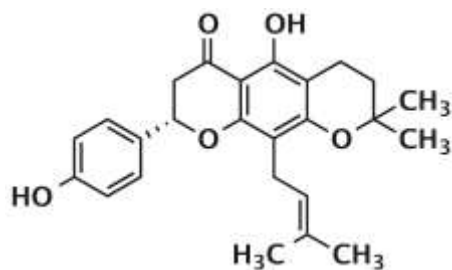


Figure 4.10 Chemical structure of lupinifolin.

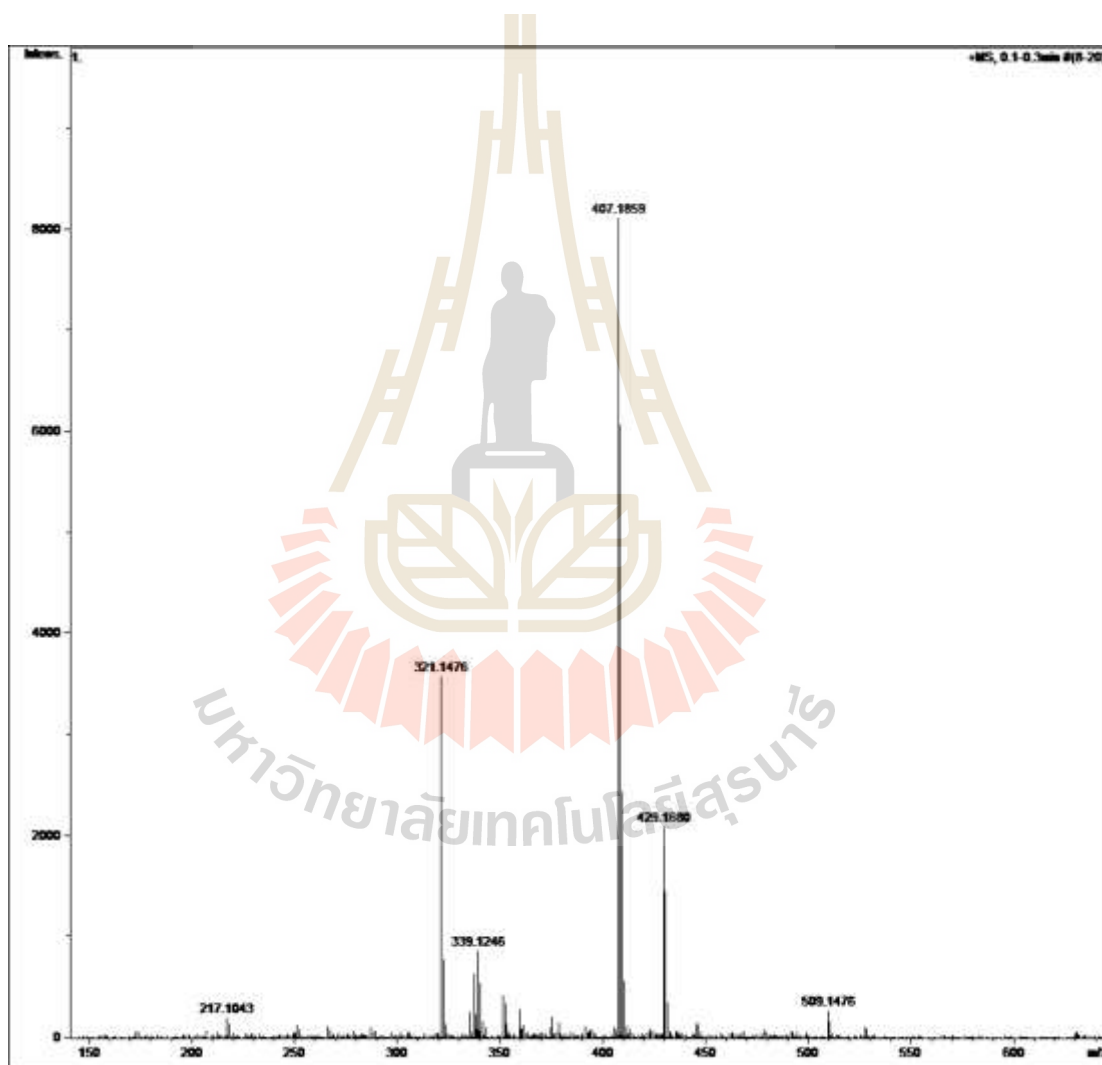


Figure 4.11 Mass spectra of lupinifolin purified from *A. myriophylla*.

4.2.2 Size, PDI and zeta potential

The lupinifolin-loaded lipid nanocarriers exhibited whitish milky colloidal (Figure 4.12). The lipid nanocarriers had a size range of 150 nm to 170 nm. Among the lipid nanocarriers, LNLC was the smallest size (151.5 ± 0.1 nm) compared to LSLN and LNE (169.5 ± 0.4 and 158.0 ± 0.2 , respectively) as shown in Table 4.3. PDI values of all lupinifolin-loaded lipid nanocarriers were about 0.2, indicating that the samples had narrow size distribution. The ZP was in the range from -29 to -41 mV. After 3 months of storage at room temperature, lupinifolin-loaded lipid nanocarriers had a minimal change in the particle size, size distribution, and surface charge. The formulations still were in colloidal form without biphasic separation.

4.2.3 Encapsulation efficiency (%EE), and loading capacity (%LC)

The fresh lupinifolin nanpcarriers exhibited encapsulation efficiency higher than 99%. The loading capacity of lupinifolin in nanocarriers was about 5% (Table 4.4). This result indicated that 100 mg of total lipid contained approximately 5 mg of lupinifolin.



Figure 4.12 Lupinifolin-loaded lipid nanocarriers.

Table 4.4 Size, PDI, zeta potential, encapsulation efficiency (%EE), and loading capacity (%LC) of lupinifolin nanocarriers.

	Size (nm)	PdI	Zeta potential (mV)	%EE	% LC
LSLN	169.5±0.4	0.222±0.010	-33.99±1.13	98.8	5.0
LNLC	151.5±0.1	0.243±0.009	-41.18±0.67	99.3	5.0
LNE	158.0±0.2	0.250±0.004	-28.91±0.81	99.3	4.9

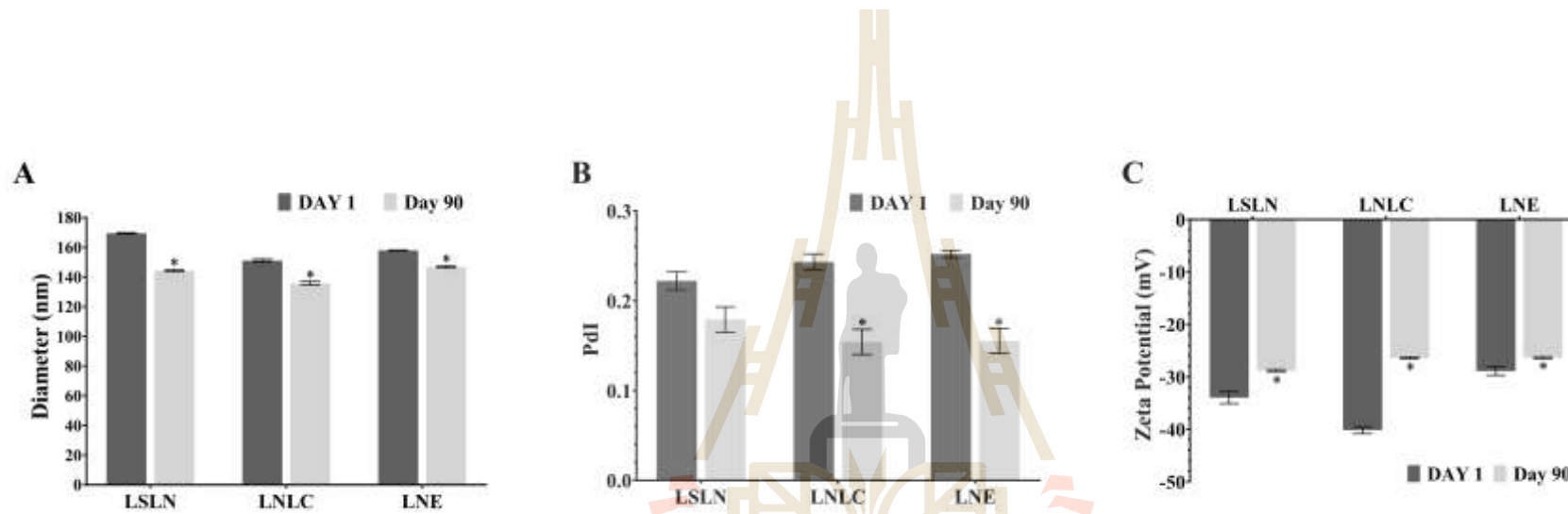


Figure 4.13 Stability of lupinifolin nanocarriers at room temperature. Size (A), PDI (B), and zeta potential (C) of QNLC after 6 months were compared with the first day of synthesis. LSLN: solid lipid nanoparticles; LNLC: nanostructured lipid carriers; LNE: lipid nanoemulsions. * $P < 0.05$, statistically significant difference.

4.2.4 *In vitro* stability in gastro-intestinal (GI) tract condition

The size of lupinifolin-loaded nanocarriers in SGF at the starting time (control) was 130-150 nm in average. The size of LSLN was increased about 30% in stomach condition whereas those of LNLC and LNE were reduced less than 15%. The size of control in SIF was in the range of 125-160 nm. The particle sizes of all lipid-based nanocarriers were significantly decreased about 12-15% in the intestinal condition (Figure 4.14).

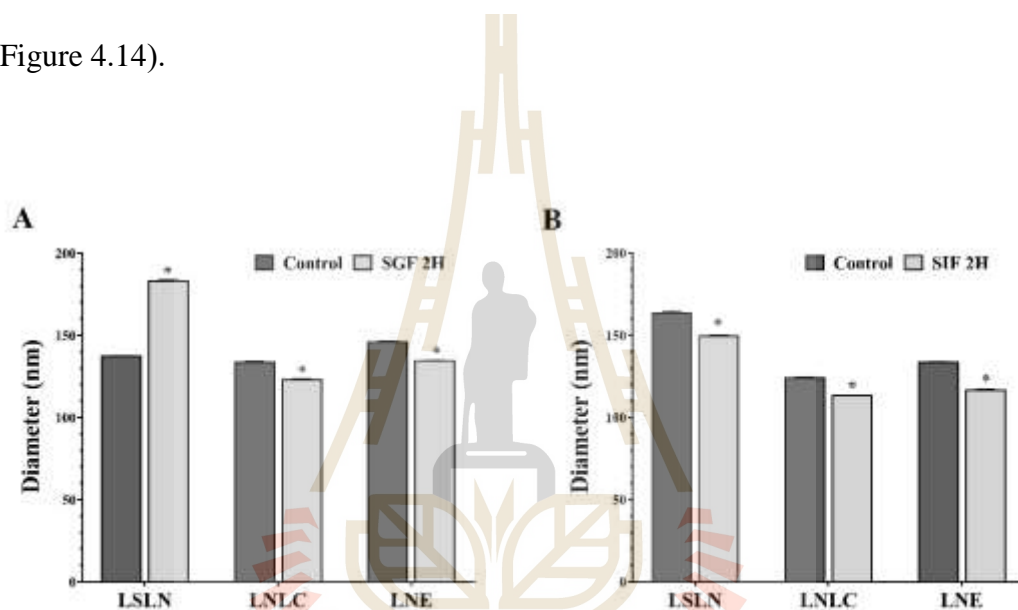


Figure 4.14 Stability of lupinifolin nanocarriers in simulated GI tract condition. The experiments were tested in simulated stomach (A) and intestinal (B) conditions. LSLN: solid lipid nanoparticles; LNLC: nanostructured lipid carriers; LNE: lipid nanoemulsions; SGF: simulated gastric fluid, SIF: simulated intestinal fluid. * $P < 0.05$, statistically significant compared with control.

4.2.5 Lupinifolin release in gastro-intestinal (GI) tract condition

Lupinifolin release from nanocarriers was investigated in SGF and SIF for 2 hours each. The release of lupinifolin from LNLC was significantly lower than that from LNE and LSLN in GI tract condition (Figure 4.15). The LSLN and LNE released free lupinifolin approximately 3 and 1.2 times higher than LNLC, respectively.

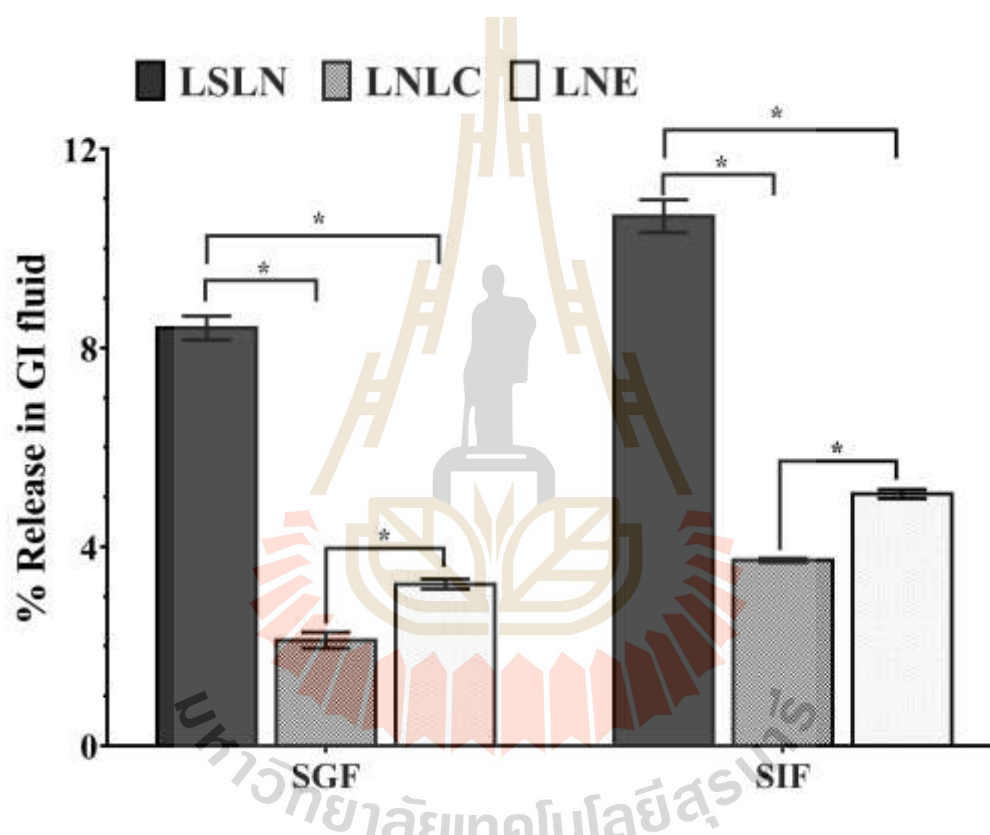


Figure 4.15 Lupinifolin release in gastro-intestinal tract condition. The released lupinifolin in SGF and SIF were measured after 4-hour incubation (2 hours each). LSLN: solid lipid nanoparticles; LNLC: nanostructured lipid carriers; LNE: lipid nanoemulsions. * $P < 0.05$, statistically significant.

4.2.6 Releasing profile

The cumulative release profiles of lupinifolin nanocarriers were determined in PBS pH 7.4 for 72 hours (Figure 4.16). LNLC exhibited lower lupinifolin release compared to LNE and LSLN with the maximum releasing rate about 21%. The LSLN and LNLC reached about 37% and 24% of lupinifolin release in 72 hours, respectively.

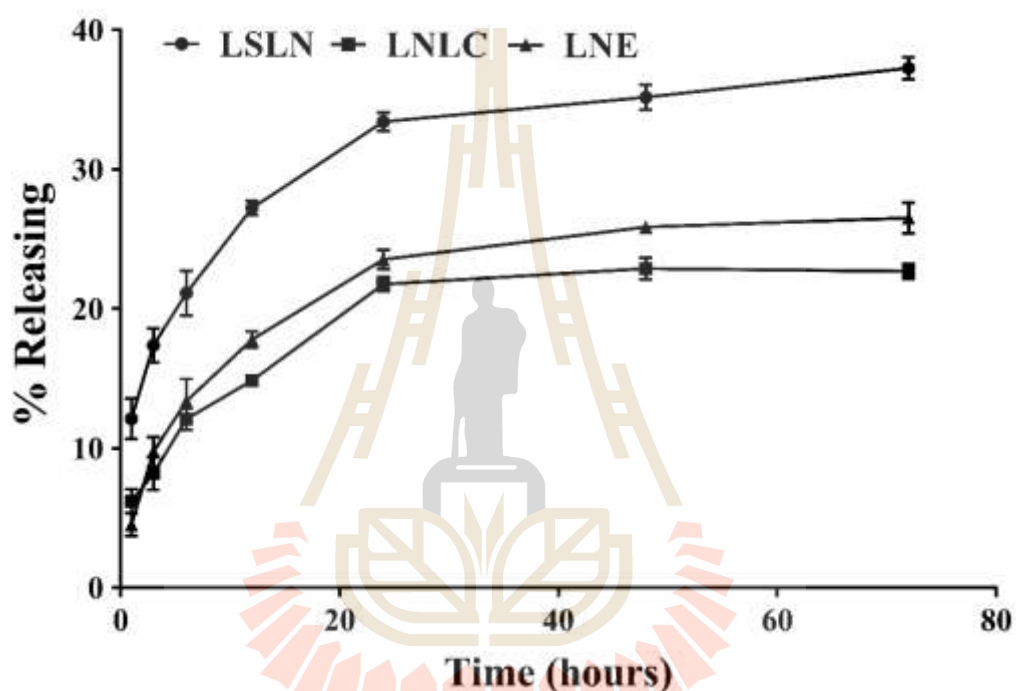


Figure 4.16 *In vitro* releasing profile of lupinifolin nanocarriers. The lupinifolin-loaded nanocarriers were incubated in PBS pH 7.4 and free quercetin releasing from nanocarriers was determined at 1, 3, 6, 12, 24, 48, 72 hours. LSLN: solid lipid nanoparticles; LNLC: nanostructured lipid carriers; LNE: lipid nanoemulsions.

4.3 *In vitro* intestinal and colonic permeability model

4.3.1 Cell culture

The passages of Caco-2 and HT29 cells used in this study were 30-45 and 21-25, respectively. They reached 80-90% confluence within 7 days, which is shown in Figure 4.17.



Figure 4.17 The confluent Caco-2 cells. The cells were photographed under microscope with 40X magnification.

4.3.2 Cell viability

4.3.2.1 The effect of quercetin and its nanocarriers on cell viability

In this study, Caco-2 cell line is the major cell for generating the triple cell co-culture monolayer model, thus the cytotoxicity was tested on this cell. The cytotoxic effects of quercetin and its nanocarriers on Caco-2 cells were investigated by MTT assay. The results demonstrated that quercetin and its NLC treatments inhibited the proliferation of Caco-2 cells in a dose-dependent manner (Figure 4.18). Caco-2 cell viability significantly dropped at 6.25 $\mu\text{g/ml}$ of QNLC-0, QNLC-1, and QNLC-3. The estimated IC_{50} values of QNLC-0, QNLC-1, and QNLC-3 were 16.57, 19.48, and 12.40 $\mu\text{g/ml}$ after 4 hours of incubation, respectively. The limit of detection (LOD) and the limit of quantification (LOQ) for quercetin were 0.1244 $\mu\text{g/ml}$ and 0.5126 $\mu\text{g/ml}$, respectively. Hence, the appropriate dose of quercetin and its nanocarriers for *in vitro* intestinal absorption model was selected at 12.5 $\mu\text{g/ml}$, which was 25 times higher than LOQ and decreased cell viability of Caco-2 cells less than 50%.

4.3.2.2 The effect of lupinifolin and its nanocarriers on cell viability

The MTT results exhibited that lupinifolin dose-dependently inhibited the proliferation of Caco-2 cells with the estimated IC_{50} value of 13.25 $\mu\text{g/ml}$ after 4 hours of incubation. The lupinifolin-loaded nanocarriers showed less toxicity on Caco-2 cells with the estimated IC_{50} value less than 1 $\mu\text{g/ml}$ after 4 hours of incubation (Figure 4.19). The LOD and LOQ of lupinifolin were 0.1066 $\mu\text{g/ml}$ and 0.4988 $\mu\text{g/ml}$, respectively. Hence, the dose of lupinifolin at 5 $\mu\text{g/ml}$, which decreased cell viability of Caco-2 cells to less than 50% and are 10 times higher than LOQ, was chosen as the proper dose for further investigation.

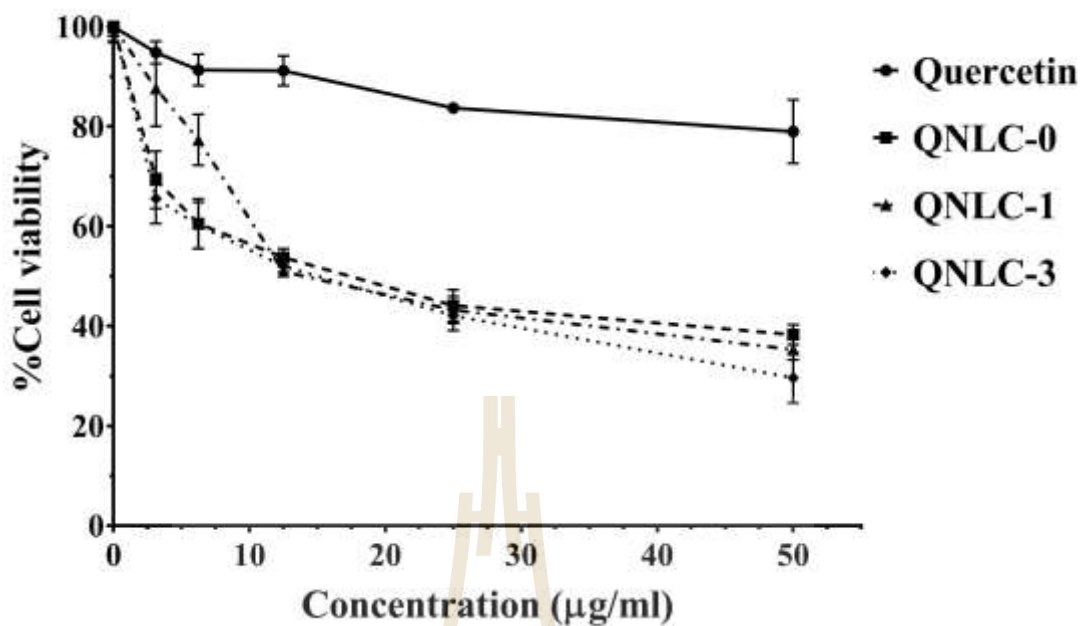


Figure 4.18 The effect of quercetin and QNLCs on cell viability of Caco-2 cells. QNLC-0: QNLC without bile salt; QNLC-1: QNLC with 5 mM bile salt; QNLC-3: QNLC with 15 mM bile salt.

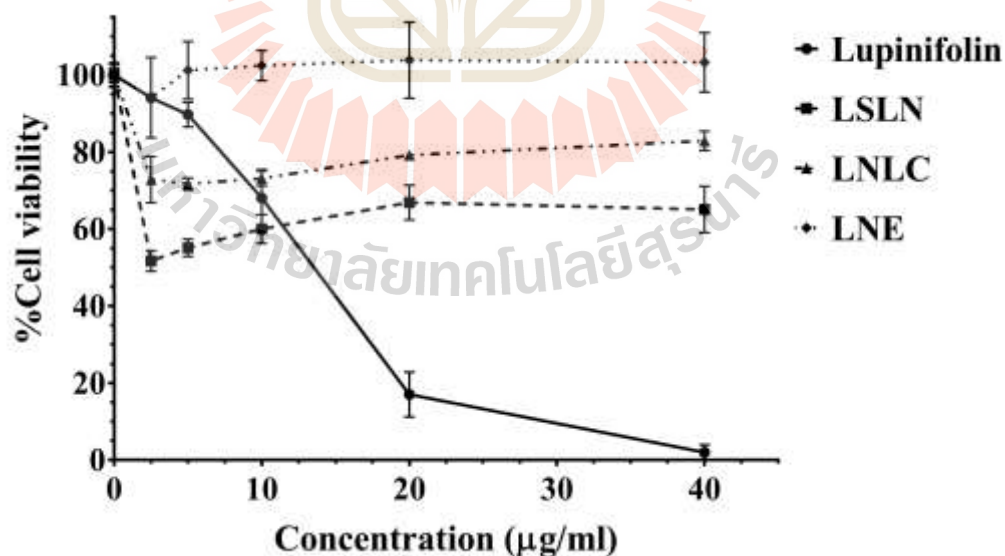


Figure 4.19 The effect of lupinifolin and its nanocarriers on cell viability of Caco-2 cells. LSLN: solid lipid nanoparticles; LNLC: nanostructured lipid carriers; LNE: lipid nanoemulsions.

4.3.3 *In vitro* transepithelial transport studies

4.3.3.1 Quercetin and its nanocarriers

The apical to basolateral transport of either quercetin or nanocarriers was measured to evaluate the intestinal absorption (Figure 4.20). The transported amount of quercetin via QNLC-0, QNLC-1, and QNLC-3 were roughly 3-4 times higher than that of native quercetin after 1-hour incubation and 5-6 times higher after 3-hour incubation.

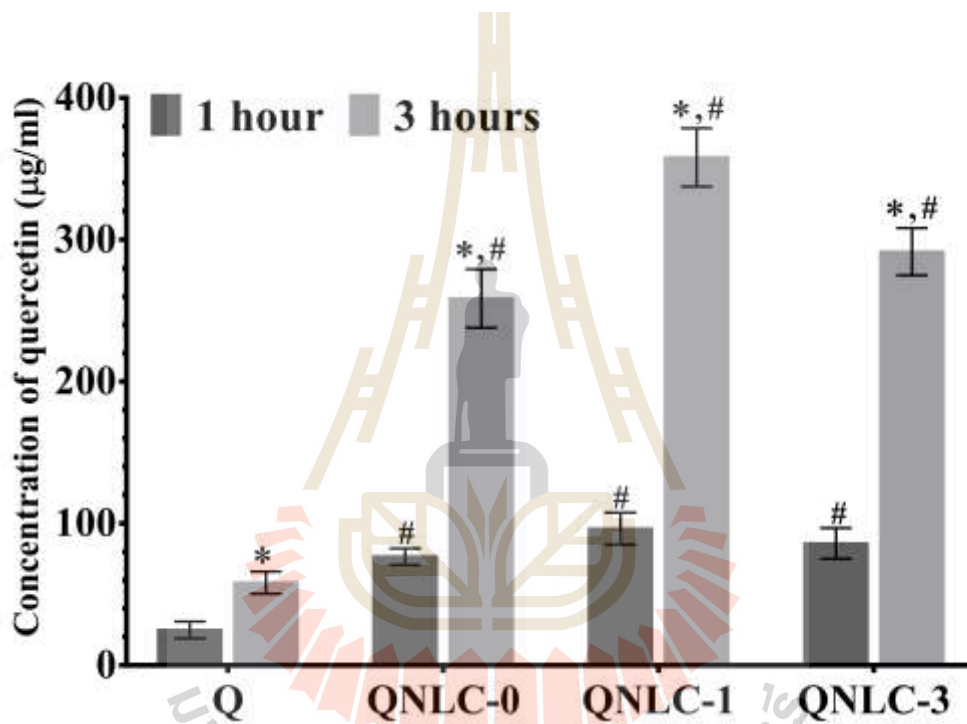


Figure 4.20 Intestinal absorption of quercetin in triple co-culture cell model. The samples from basolateral side were measured with HPLC (mean±SEM, n=6) after incubation with quercetin and its nanocarriers (20 µg/ml), Q: native quercetin; QNLC-0: QNLC without bile salt; QNLC-1: QNLC with 5 mM bile salt; QNLC-3: QNLC with 15 mM bile salt at 37 °C for 1 h and 3 h. * $P < 0.05$ compared with 1-hour incubation in the same treatment, # $P < 0.05$ compared with native quercetin.

4.3.3.2 Lupinifolin and its nanocarriers

The amounts of lupinifolin, which transported to basolateral side of the triple co-culture cell model, could not be evaluated with HPLC after incubation up to 3 hours (Table 4.5). The results showed that area under the curve of lupinifolin in all samples were less than the minimal average area of standard curve, thus they were calculated comparatively as negative values. Hence, *in vitro* transepithelial transport model may not be appropriate for studying the intestinal absorption of lupinifolin.

Table 4.5 HPLC results of lupinifolin on *in vitro* intestinal absorption model.

Area (mAU*s)				Comparative concentration of lupinifolin ($\mu\text{g/ml}$)			
Lupinifolin	LSLN	LNLC	LNE	Lupinifolin	LSLN	LNLC	LNE
15.4	13.9	47.1	32.9	-0.47	-0.49	-0.15	-0.29
14.3	16.3	51.9	28.3	-0.48	-0.46	-0.10	-0.34
17.7	18.0	43.1	24.8	-0.45	-0.44	-0.19	-0.38
21.8	22.9	50.1	50.2	-0.20	-0.09	-0.12	-0.12
26.0	26.6	52.4	45.4	-0.06	-0.05	-0.10	-0.17
26.8	25.2	52.0	52.1	-0.36	-0.17	-0.10	-0.10

4.4 *Ex vivo* intestinal absorption

4.4.1 Quercetin and its nanocarriers

The concentrations of quercetin absorbed from the native quercetin and its QNLCs through the intestinal sac are shown in Figure 4.21. The results indicate that the absorption of quercetin from QNLCs was enhanced in all intestinal segments. No significant differences were observed in terms of quercetin absorption between the QNLCs in the duodenum, whereas the intestinal permeability of quercetin from QNLCs with bile salts (QNLC-1 and QNLC-3) were significantly increased in the jejunum and ileum compared with that from QNLC without bile salts (QNLC-0). The jejunum was the optimal site for quercetin absorption from QNLC-1 and QNLC-3, which was about 12-14 times higher than those from the native quercetin.

4.4.2 Lupinifolin and its nanocarriers

The lupinifolin absorption through the intestinal segments were investigated and the results were shown in Figure 4.22. Lupinifolin-loaded lipid nanocarriers enhanced the absorption of lupinifolin in three intestinal segments. The intestinal permeability of lupinifolin nanocarriers had no significant differences in the duodenum and ileum. On the contrary, the absorption of lupinifolin from LNLC and LNE were significantly increased in the jejunum with 14-18 times higher than that from the native lupinifolin. Hence, the suitable location for lupinifolin absorption is jejunum.

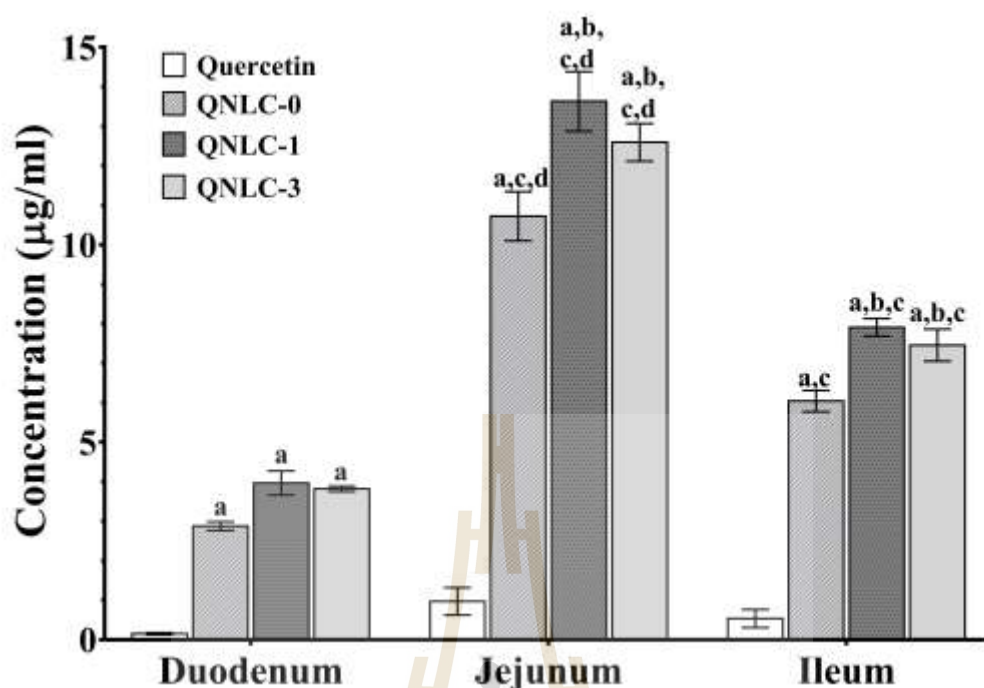


Figure 4.21 *Ex vivo* intestinal absorption of quercetin. Concentrations of quercetin in different small intestine segments were investigated after one-hour incubation with quercetin solution (50 µg/ml), QNLC-0: QNLC without bile salt, QNLC-1: QNLC with 5 mM bile salt, and QNLC-3: QNLC with 15 mM bile salt at 37 °C for 1 hour. a: significant differences compared to native quercetin in the same segment ($P < 0.05$), b: significant differences compared to QNLC-0 in the same segment ($P < 0.05$), c: significant differences compared to each type of nanocarriers in duodenum segment ($P < 0.05$), d: significant differences compared to each type of nanocarriers in ileum segment ($P < 0.05$).

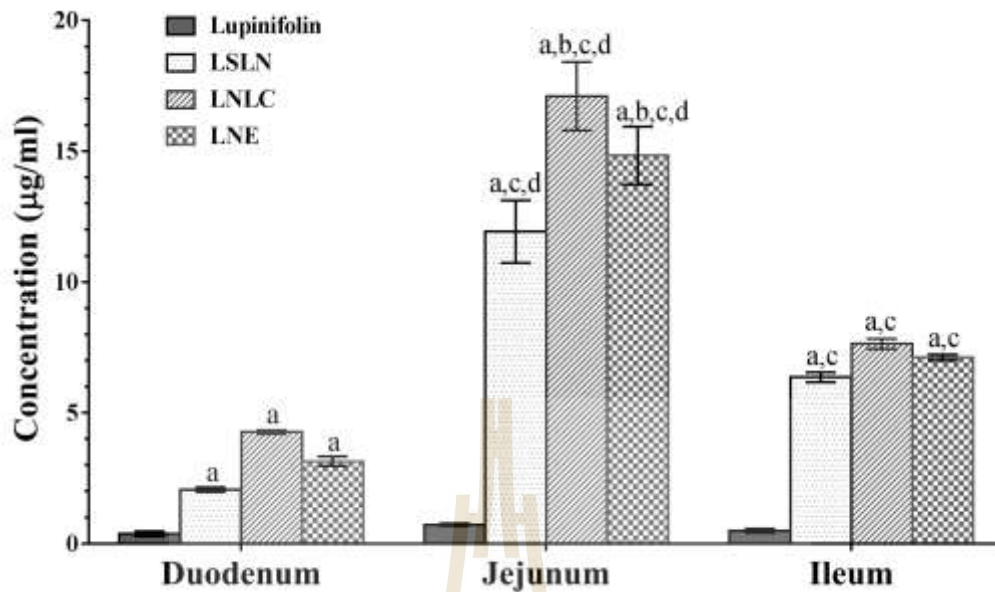


Figure 4.22 *Ex vivo* intestinal absorption of lupinifolin. Concentrations of lupinifolin in different small intestine regions were measured after one-hour incubation in lupinifolin solution (50 µg/ml), solid lipid nanoparticles (LSLN), nanostructured lipid carriers (LNLC), and lipid nanoemulsions (LNE) at 37 °C for 1 hour. a: significant differences compared to lupinifolin suspension in the same segment ($P < 0.05$), b: significant differences compared to LSLN in the same segment ($P < 0.05$), c: significant differences compared to each type of nanocarriers in duodenum segment ($P < 0.05$), d: significant differences compared to each type of nanocarriers in ileum segment ($P < 0.05$).

CHAPTER V

DISCUSSION AND CONCLUSION

Plenty of factors have an impact to the effectiveness of medicinal treatment including pharmacokinetic and pharmacodynamic properties of drug, pharmaceutical dosage form, age, gender, circadianrhythms, intestinal bacteria, pathophysiological conditions, and xenobiotics pharmaceutical dosage form (Babiloni et al., 2013; Colalto, 2010; Hussein et al., 2013; Lohr, Willsky, and Acara, 1998; Otsubo, 2015). Absorption is the key factor in drug efficacy and therapy result. The major problems of herbal medicines especially flavonoids are their poor solubility, negligible permeability, instability, and consequently low bioavailability (Anitha et al., 2011; Cai et al., 2013; Chansuwan et al., 2016; Cragg and Newman, 2005; Monache et al., 1995; Moorthi and Kathiresan, 2013; Schneider et al., 2015). Not only those properties affect to drug absorption, but they also are the cause of their decreased efficacy. The development of drug delivery system plays an important role for enhancing of flavonoid absorption in the oral administration. In this study, two flavonoids (quercetin and lupinfolin) were chosen as models of choices for developing nanoscale carriers, which based on lipid materials.

Quercetin were encapsulated into lipids with bile salts and sonicated to generate nano-sized particles. Three types of formulated quercetin-loaded lipid nanocarriers, QNE, QSLN, and QNLC, were different in physical state of lipid, which were liquid lipid, solid lipid, and solid-liquid lipid, respectively. The two formulations

of QNEs (QNE-0 and QNE-1) exhibited a translucent yellowish emulsion, meanwhile the other two formulations, QNE-2 and QNE-3, displayed a transparent yellowish emulsion (Figure 4.1). The appearance of emulsion depends on the average size of particles. Even though the sizes of the translucent QNEs are higher than 100 nm, those of the transparent QNEs are lower than 100 nm (Li et al., 2009). These results are accordance with emulsion appearances from the previous reports (Aditya et al., 2014; Md et al., 2018). However, all QNEs were unstable and separated into two phases during storage at room temperature for 3 months. There are at least two possible reasons which cause the changing of the particle size. First is the composition of the lipid core (essential clove oil), which can vaporize, subsequently making QNEs have unappropriated ratio of stabilized agents (Y. Liu and Feng, 2015; Yostawonkul et al., 2017). The second is the high polydispersity index (PdI) of QNEs (>0.3), which impacts the stability of particle sizes as seen in Figure 4.2 (Danaei et al., 2018). QSLN formulations (Figure 4.3) were also instability and became biphasic separation within a day due to less stabilizing agents compared to the large amount of solid lipid core. In contrast, the QNLCs (Figure 4.4) were the best formulation based on their stability during storage at room temperature for 3 months.

The liquid lipid component of QNLC1, QNLC2, and QNLC3 is the volatile clove oil, but used in different ratio between liquid and solid lipids. The mechanism underlying their instability and two-phase separation within a week is the same as that for QNEs, so olive oil was used as the liquid lipid to formulated QNLC4 instead of the essential clove oil. The proportion between liquid and solid lipids was 1:4, which is suggested for the production of NLC by several studies (Aditya et al., 2014; Chinsriwongkul et al., 2012). The QNLC4 formulations contained different

concentrations of bile salts (sodium cholate hydrate), which can enhance the drug absorption by disruption interfacial regions of the phospholipid vesicles and thus the phospholipids can diffuse faster to the interface (Salminen et al., 2014). Some publication has reported that drug conjugated with bile acids can bind with intestinal bile-acid transporters, probably increasing its absorption via gastro-intestinal tract (Mirvish, 1964; Park et al., 2006). Another report showed that the bile acid combined with the derivative of heparin could improve the drug absorption through intestinal epithelial cells (Park et al., 2007). Moreover, taurocholic acid (another type of bile salts) was also demonstrated to elevate the absorption of drug-encapsulated nanoparticles by bile-acid transporters (Khatun et al., 2014; Tian et al., 2017). Therefore, a suitable concentration of bile salts was investigated to produce a stable QNLC in this study. The following results of QNLC4 will be described as the properties of “QNLC”.

The stability of nanocarriers can be predicted from the average diameter (particle size), size distribution (PdI), and surface charge of particles (zeta potential). A translucent yellowish dispersion (Figure 4.4) is the appearance of fresh QNLCs, which can reflect the small size, monodisperse distribution of size, and negative surface charge of nanoparticles as presented in Table 4.2. These Physicochemical characterizations of QNLCs indicated their stability during storage. Figure 4.5 illustrates the results of QNLCs' stability. No significant changes were observed for 3 months after synthesis, when QNLC-3 were stored at room temperature. All QNLCs showed no separation into two phases with a tiny increase in size. The QNLC formulations were found to have encapsulation efficiency higher than 99%. The loading capacity of quercetin has been reported to be lower than 1% in all lipid nanocarriers which were synthesized from different laboratories (Aditya et al., 2014; Pool, Mendoza, Xiao, and McClements,

2013). The quercetin loading capacity of QNLCs in this study (0.5%) was similar to those reported in these previous studies.

The stability of lipid nanocarriers was further investigated under *in vitro* gastro-intestinal condition. In the case of drug degradation protection, the lipid nanocarriers should maintain their stability in the stomach until they reach intestine. When the particles reached the small intestine, they would be digested by intestinal enzyme complex to form mixed micelles, thereby enhancing its bioaccessibility and bioavailability (Aditya et al., 2014; Pool et al., 2013). However, in the present study, drug delivery systems were designed to increase drug solubility and enhance absorption through GI tract by nano-scale carriers. Thus, no or minimal drug release in GI tract condition was the goal of drug designs. It was found that after digestion, the size of QNLCs became larger under simulated stomach and smaller under intestinal conditions which occurred in other studies as well (Aditya et al., 2014; Tan et al., 2012). As seen in Figure 4.6A, the particle sizes of QNLC-1 which contained low concentration of bile salts were changed less than those of QNLC-2 and QNLC-3. The disruption of bile salts to interfacial regions of lipid particles may attribute to the high degree of changes in the particle sizes of QNLC-2 and QNLC-3 (Pool et al., 2013).

The influence of bile salts to the releasing property of quercetin in the GI tract was studied in simulated GI tract condition. QNLC with low and high concentrations of bile salt (QNLC-1 and QNLC-3, respectively) and QNLC without bile salts (QNLC-0) were compared in this experiment. The addition of bile salt to QNLC formulation may cause instability particle sizes as described above, but it had no effect to the releasing property in the GI tract. From Figure 4.7, the results showed no significant alteration in quercetin release in GI tract among three formulations of QNLCs because

their physical state and compositions of lipid remained the same. The release of QNLC-0 in the GI tract was similar to QNLC-1 and QNLC-3 in both simulated gastric fluid (SGF) (about 7%) and simulated intestinal fluid (SIF) (about 16%). The release of quercetin from QNLCs, which was higher in SIF than in SGF may be due to the pancreatin which containing lipase enzyme in SIF. In this study, QNLCs were composed of olive oil, which is medium chain triglyceride (MCT) and can be digested into medium chain free fatty acids, resulting in the release of drug from lipid nanocarriers. In contrast, long chain triglycerides have been reported to inhibit activity of lipase (Aditya et al., 2014; Silva et al., 2014). Any lipid nanocarriers, which comprise long chain triglycerides, may have a slower drug release in SIF.

The *in vitro* releases of quercetin from the QNLCs in PBS 7.4 were determined by using a dialysis bag. QNLC-0 showed lower releasing rate compared to QNLC-1 and QNLC-3 in all time intervals (Figure 4.8). The results implied that QNLCs exhibited sustained release in the circulation system. In the previous studies, the *in vitro* and *in vivo* release of nanocarriers were extended until reach 90% within 30-35 days (Shen and Burgess, 2015; Zhang et al., 2007). Hence, these lipid nanocarriers may reach 90-100% releasing within a month. There are enzymes name lipoprotein lipase (LDL) could digested the lipid of nanocarriers and release quercetin into target organs. The lipoprotein lipase, which is found at capillaries and various organs, plays an important role in breaking down of lipid in the form of triglycerides (Mead, Irvine, and Ramji, 2002).

The purified lupinifolin was obtained as yellow needle-shaped crystal by crystallization from the hexane extract at room temperature. In the crystallization process, lupinifolin were concentrated and saturated by heating. The saturated solution

was gradually crystallized into yellow needle-shape crystal whereas the impurities remain in the hexane. The techniques of flavonoid extraction from medicinal plants are based on the non-polar solvents, heating, and mixing. Soxhlet extraction is the most extensively and regularly used for the extraction of natural products (Gurib-Fakim, 2006). In order to get purified lupinifolin, dried stems of *A. myriophylla* Benth were extracted with hexane using soxhlet apparatus, which yield about 2.5 mg of lupinifolin/g of dried stem. The purity of lupinifolin was more than 95% based on the NMR spectrum, which is consistent with a previous report (Mahidol et. al., 1997) and its molecular formula was also confirmed by mass spectrometry. Lupinifolin bioavailability has never been investigated in clinical trial or animal experiment. Due to its poor solubility similar to several plant flavonoids such as curcumin (Schneider et al., 2015), lupinifolin possibly exhibits low oral bioavailability. In this research, lupinifolin was successful encapsulated by lipid materials for delivery system.

The freshly prepared lupinifolin-loaded lipid nanocarriers have the appearance of white homogeneous milky solution. The results from Table 4.4 reveals that freshly prepared lipid nanocarriers had a size range from 150 nm to 170 nm. Among the lipid nanocarriers, the particle size of LNLC was the smallest (151.5 ± 0.1 nm) compared to LSLN and LNE (169.5 ± 0.4 and 158.0 ± 0.2 , respectively). Probe sonication was applied to decrease size of the emulsion droplets to accomplish in the nanometer range, smaller than 200 nm. This size of particles is large enough to avert the puncture from blood capillaries and small enough to avoid the seizure of macrophages in the reticuloendothelial system, and thus bypass liver and spleen filtration (Jawahar et al., 2012). Nanoparticles with the size less than 200 nm enter cells by endocytosis and are excreted from the cells through the exocytosis pathway (Hussein et al., 2013). It is

evident that composition of the lipid has no significant impact on the size of the nanocarriers, whereas physical state has prominent influences. Dynasan[®]116 in LSLN and MCT in LNE, which are composed of triglyceride, have different sizes. Moreover, significant size reduction of LNLC, which were fabricated using mixture of solid and liquid lipids in the present study was observed. In addition, the reason may be because crystalline lipid core of LSLN is bigger than amorphous core of LNLC and LNE. However, this synopsis is opposite to the discussion of Aditya et al. (2014), which suggested that the compositions of lipid (mono-, di-, and triglyceride) play more important role. In previous studies, the component analysis of NLC indicated that the bioavailability is enhanced by the solid and liquid lipids which were similar to fat food. The secretion of bile in the small intestine could be induced these lipids and the drug-loaded NLC interact with bile salts to process mixed micelles. These micelles helped in permeation of the whole NLC to the lymphatic system with avoiding the first pass effect via liver metabolism. (Khalil, El-bary, Kassem, Ghorab, and Ahmed, 2013; Khan et al., 2015; Rostami et al., 2014; Suhailah and Arabia, 2014).

As demonstrated in Table 4.4 the size distributions of all lupinifolin-loaded lipid nanocarriers as determined by dynamic light scattering (DLS) achieve polydispersity index (PdI) of about 0.2, which indicates acceptable monodispersity (PdI 0.1-0.3) (Sáenz and Asua, 1995). The good monodispersity associates with narrow particle-size distribution, which results in drug absorption efficiency of nanoparticles and absence of phase separation (Muzzarelli, 2011). The zeta potential (ZP) of all formulations of lupinifolin, which reflects surface charge properties of particles, was in the range of -29 mV to -41 mV. The ZP change of the nanoparticle surface could lead to aggregation upon storage condition (Müller and Eckhardt, 1978). Colloids will be

instability if their ZPs are from ± 10 mV to ± 30 mV, and become rapid coagulation if the ZPs are between 0 to ± 10 mV (Hanaor, Michelazzi, Leonelli, and Sorrell, 2012; O'Brien, Midmore, Lamb, and Hunter, 1990). The encapsulation efficiency of fresh formulations had shown higher than 99%. The lupinifolin loading capacity in lupinifolin-loaded nanocarriers was about 5%. In this study, lipid nanocarriers were prepared with a constant lipid concentration of 10.0% (w/w). From literature, it has no evidence that physical state of the lipid significant effect on drug encapsulation, whereas all formulations composed of high triglyceride effected on equivalent loading and stability in GI tract (Aditya et al., 2014).

The effect of lipid physical state on stability of nanocarriers was explored with *in vitro* GI simulation. As mentioned earlier, the perfect protective lipid carriers should be stable or less leakage in the stomach until it reaches small intestine in order to enhance their bioaccessibility and bioavailability. They will be formed mixed micelles due to digestion of intestinal enzyme (lipid degradation products, bile salts and phospholipids) (Aditya et al., 2014; Bilia et al., 2014). In stomach condition, the size of LSLN produced in this study was significant increased while LNLC and LNE were minor decreased. All lipid nanocarriers were stable in an intestinal condition with modest significant decreasing (Figure 4.14). Nonetheless, some previous literatures suggested that the size of lipid nanocarriers could be changed under pH stress of GI conditions (Aditya et al., 2014; Tan et al., 2012). LSLN is high in saturated fat of Dynasan[®]116 which can crystalline into bigger particle.

Lupinifolin release in the GI tract was low in LNLC compared to LSLN and LNE in both stomach and intestine condition (Figure 4.15). Since drug release of LNLC in the GI tract is less and sustained release in GI tract, this indicated that it is a good

candidate to enhance intestinal permeability. Regarding to the effect of physical state of the lipids, lipid molecule in LSLN is arranged more densely and tightly than that in LNLC and LNE, which might limit the surface change of SLN, resulting in reduced hydrolysis rate and hydrolyzing capacity (Salminen et al., 2014). The release of lupinifolin was investigated in PBS pH 7.4 to predict the releasing rate in blood condition. LNLC showed lower releasing rate compared to LNE and LSLN in all time intervals (Figure 4.16). All the three types of lupinifolin-loaded lipid nanocarriers exhibited sustained release pattern without any burst release. Due to the stability and releasing profile, LNLC had the best chance to be detected in further *ex vivo* experiment.

The best candidate quercetin-loaded nanocarriers (QNLC-0, QNLC-1 and QNLC-3) and lupinifolin-loaded lipid nanocarriers (LSLN, LNLC, and LNE) were selected to compare their abilities of transepithelial transportation. The Caco-2 cells of *in vitro* triple co-culture cells were induced to generate microfold cells (M cells) of the Peyer's patches by Raji B cells (Lozoya-Agullo et al., 2017). In addition to transportation through paracellular diffusion of lipid nanocarriers, it also can penetrate across M cells (Jawahar et al., 2012; Mukhopadhyay and Prajapati, 2015). The results showed that QNLC-1 can be transported about 6 times higher than native quercetin within 3 hours (Figure 4.20). However, the concentrations of the initial lupinifolin and its nanocarriers which showed no toxic to cells were too low to be detect in basolateral side (Table 4.5). Hence, the intestinal absorption of lupinifolin and its nanocarrier needed an *ex vivo* intestinal absorption test.

After ingestion, lipid nanocarriers can be absorbed from the GI tract into circulatory system by several pathways: paracellular diffusion or penetrate through

tight junction (Tan et al., 2012), transportation through specialized M cells and other mucosa associated lymphoid tissues (MALT) by phagocytosis, receptor-mediated endocytosis and transcytosis into lymphatic systems (Jawahar et al., 2012; Mukhopadhyay and Prajapati, 2015), and mixed micelles by enterocytes along with acid pathway (Bilia et al., 2014). In an *ex vivo* absorption of quercetin, QNLC without bile salts (QNLC-0) and QNLC with low and high bile salts (QNLC-1 and QNLC-3, respectively) were compared to native quercetin. The results in Figure 4.21 revealed that QNLCs exhibited the significant enhancement in all intestinal segments. However, the jejunum appeared to be the optimal site for quercetin absorption from QNLC with bile salt combination (QNLC-1 and QNLC-3). The absorption of quercetin from nanocarriers was about 12-14 times higher than that from native quercetin. The *ex vivo* result of QNLCs is consistent to *in vitro* transepithelial model, which composes of a lot of the Peyer's patches like in the jejunum segment.

Like the results of quercetin-loaded nanocarriers, the concentrations of absorbed lupinifolin through *ex vivo* small intestine (Figure 4.22) indicated that the lupinifolin absorption from lipid nanocarriers was enhanced in the three intestinal segments. No significant differences were observed in term of lupinifolin absorption among lipid nanocarriers in the duodenum and ileum, while the intestinal permeability of lupinifolin from LNLC and LNE were significantly increased in the jejunum compared to that from LSLN. Similar to quercetin, the jejunum was the optimal site for lupinifolin absorption from lipid nanocarriers, which was 12-16 times higher than that from native lupinifolin. It is most likely that the small size of LNLC and LNE enabled higher permeate through the membrane via Peyer's patches during transportation, thereby optimizing intestinal absorption and permeation.

In conclusion, nanocarriers were successfully fabricated as delivery systems for quercetin and lupinifolin to enhance their oral bioavailability. The enhancement in permeability and absorption from the GI tract was proved in both *in vitro* and *ex vivo* systems. The characteristics of the best quercetin- and lupinifolin-loaded nanocarriers synthesized from the present study are summarized as Table 5.1.

These QNLC with 5 mM bile salts and LNLC formulations are recommended for further *in vivo* studies because of their small sizes, stability in GI fluid, possible sustained release in circulation system, and good absorption through small intestine.

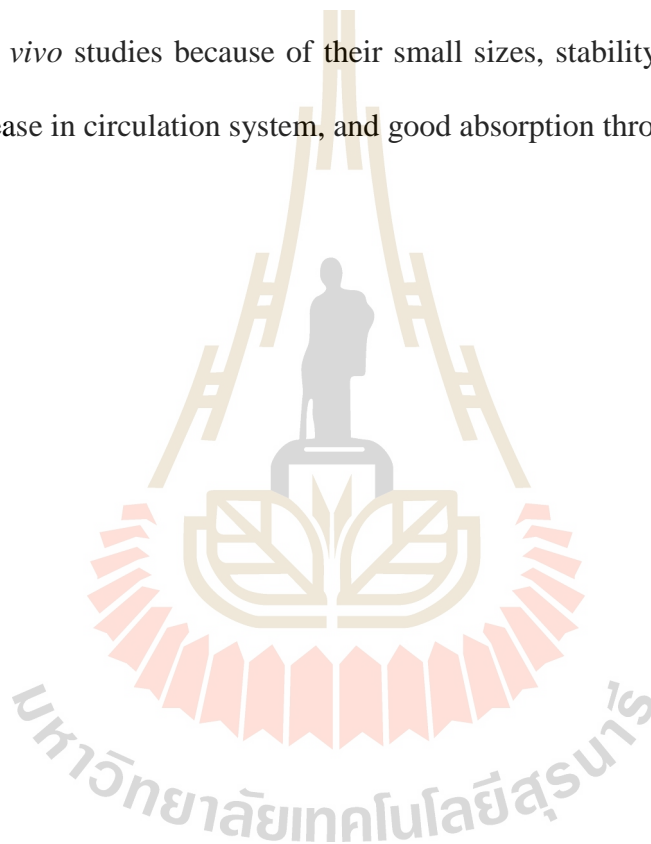


Table 5.1 The characteristics of the best quercetin- and lupinifolin-loaded nanocarriers.

Characteristics	Quercetin-loaded lipid nanocarriers	Lupinifolin-loaded lipid nanocarriers
Type	Nanostructure lipid carriers (NLCs) with bile salts	Nanostructure lipid carriers (NLCs)
Composition		
<i>Solid lipid</i>	Glycerol monostearate (GMS)	Dynasan®116
<i>Liquid lipid</i>	Olive oil	Medium chain triglyceride (MCT)
Size (nm)	115.5±2.0	151.5±0.1
Polydispersity index	0.200±0.011	0.243±0.009
Zeta potential	-41.12±0.38	-41.18±0.67
Encapsulation efficiency	99.5%	99.3%
Loading capacity	0.5%	5.0%
Release in GI tract	16.2%	3.7%



REFERENCES

มหาวิทยาลัยเทคโนโลยีสุรนารี

REFERENCES

- Aditya, N. P., Macedo, A. S., Doktorovova, S., Souto, E. B., Kim, S., Chang, P. S., and Ko, S. (2014). Development and evaluation of lipid nanocarriers for quercetin delivery: A comparative study of solid lipid nanoparticles (SLN), nanostructured lipid carriers (NLC), and lipid nanoemulsions (LNE). **LWT-Food Science and Technology**. 59(1): 115–121.
- Anitha, A., Deepagan, V. G., Divya Rani, V. V., Menon, D., Nair, S. V., and Jayakumar, R. (2011). Preparation, characterization, *in vitro* drug release and biological studies of curcumin loaded dextran sulphate-chitosan nanoparticles. **Carbohydrate Polymers**. 84(3): 1158–1164.
- Ansaria, M. A., Abdula, H. M., Joshia, G., Opii, W. O., and Butterfield, D. A. (2009). Protective effect of quercetin in primary neurons against $A\beta$ (1-42): relevance to Alzheimer's disease. **Journal of Nutrient Biochem**. 20(4): 269–275.
- Babiloni, C., Infarinato, F., Aujard, F., Bastlund, J. F., Bentivoglio, M., Bertini, G., Percio, C. D., Fabene, P. F., Forloni, G. H., Ezquerro, M. T., Noè, F. M., Pifferi, F., Ros-Bernal, F., Christensen, D. Z., Dix, S., Richardson, J. C., Lamberty, Y., Drinkenburg, W., and Rossini, P. M. (2013). Effects of pharmacological agents, sleep deprivation, hypoxia and transcranial magnetic stimulation on electroencephalographic rhythms in rodents: towards translational challenge models for drug discovery in Alzheimer's disease. **Clinical Neurophysiology**. 124(3): 437–451.

- Bahari, L. A. S., and Hamishehkar, H. (2016). The impact of variables on particle size of solid lipid nanoparticles and nanostructured lipid carriers ; A comparative literature review. **Tabriz University of Medical Sciences**. 6(2): 143–151.
- Bilia, A. R., Isacchi, B., Righeschi, C., Guccione, C., and Bergonzi, M. C. (2014). Flavonoids loaded in nanocarriers : An opportunity to increase oral bioavailability and bioefficacy. **Food and Nutrition Sciences**. 5(July): 1212–1227.
- Cai, X., Fang, Z., Dou, J., Yu, a, and Zhai, G. (2013). Bioavailability of quercetin: problems and promises. **Current Medicinal Chemistry**. 20: 2572–2582.
- Chansuwan, S., Palanuvej, C., and Ruangrunsi, N. (2016). **Pharmacognostic specification and lupinifolin content of *Derris reticulata* stem wood**. Proceedings of the 8th Thailand-Japan International Academic Conference. Tokyo, Japan, 29 October 2016. pp 214–219
- Chen, Z., Sun, J., Chen, H., Xiao, Y., Liu, D., Chen, J., Cai, H., and Cai, B. (2010). Comparative pharmacokinetics and bioavailability studies of quercetin, kaempferol and isorhamnetin after oral administration of *Ginkgo biloba* extracts, *Ginkgo biloba* extract phospholipid complexes and *Ginkgo biloba* extract solid dispersions in rats. **Fitoterapia**. 81: 1045–1052.
- Chinsriwongkul, A., Chareanputtakhun, P., Ngawhirunpat, T., Rojanarata, T., Sila-on, W., Ruktanonchai, U., and Opanasopit, P. (2012). Nanostructured lipid carriers (NLC) for parenteral delivery of an anticancer drug. **Journal of the American Association of Pharmaceutical Scientists**. 13(1): 150–158.
- Chirio, D., Gallarate, M., Peira, E., Battaglia, L., Muntoni, E., Riganti, C., Biasibetti, E., Capucchio, M. T., Valazza, A., Panciani, P., Lanotte, M., Annovazzi, L., Caldera, V., Mellai, M., Filice, G., Corona, S., and Schiffer, D. (2014). Positive-

- charged solid lipid nanoparticles as paclitaxel drug delivery system in glioblastoma treatment. **European Journal of Pharmaceutics and Biopharmaceutics**. 88(3): 746–758.
- Choi, K.-O., Choe, J., Suh, S., and Ko, S. (2016). Positively charged nanostructured lipid carriers and their effect on the dissolution of poorly soluble drugs. **Molecules**. 21(5): 672.
- Colalto, C. (2010). Herbal interactions on absorption of drugs: Mechanisms of action and clinical risk assessment. **Pharmacological Research**. 62(3): 207–227.
- Cragg, G. M., and Newman, D. J. (2005). Plants as a source of anti-cancer agents. **Journal of Ethnopharmacology**. 100(1–2): 72–79.
- Danaei, M., Dehghankhold, M., Ataei, S., Hasanzadeh Davarani, F., Javanmard, R., Dokhani, A., Khorasani, S., and Mozafari, M. R. (2018). Impact of particle size and polydispersity index on the clinical applications of lipidic nanocarrier systems. **Pharmaceutics**. 10(2): 1–17.
- Das, S., and Chaudhury, A. (2011). Recent advances in lipid nanoparticle formulations with solid matrix for oral drug delivery. **Journal of the American Association of Pharmaceutical Scientists**. 12(1): 13–15.
- Derakhshandeh, K., Hochhaus, G., and Dadashzadeh, S. (2011). *In-vitro* cellular uptake and transport study of 9-nitrocamptothecin PLGA nanoparticles across Caco-2 cell monolayer model. **Iranian Journal of Pharmaceutical Research**. 10(3): 425–434.
- Dilnawaz, F., and Sahoo, S. K. (2013). Enhanced accumulation of curcumin and temozolomide loaded magnetic nanoparticles executes profound cytotoxic effect in glioblastoma spheroid model. **European Journal of Pharmaceutics and**

Biopharmaceutics. 85(3 PART A): 452–462.

- Ferry, R. (1996). Phase I clinical trial of the flavonoid tyrosine kinase quercetin : Pharmacokinetics for *in vivo*. **Clinical Cancer Research.** 2(April): 659–668.
- Ghosh, A., Sarkar, S., Mandal, A. K., and Das, N. (2013). Neuroprotective role of nanoencapsulated quercetin in combating ischemia-reperfusion induced neuronal damage in young and aged rats. **PLoS ONE.** 8(4): e57735.
- Graefe, E. U., Wittig, J., Mueller, S., Riethling, A., Uehleke, B., Drewelow, B., Pforte, H., Jacobasch, G., Derendorf, H., and Veit, M. (2001). Pharmacokinetics and bioavailability of quercetin glycosides in humans. **Journal of Clinical Pharmacology.** 41: 492–499.
- Gurib-Fakim, A. (2006). Medicinal plants: Traditions of yesterday and drugs of tomorrow. **Molecular Aspects of Medicine.** 27(1): 1–93.
- Hanaor, D., Michelazzi, M., Leonelli, C., and Sorrell, C. C. (2012). The effects of carboxylic acids on the aqueous dispersion and electrophoretic deposition of ZrO₂. **Journal of the European Ceramic Society.** 32(1): 235–244.
- Hussein, M. Z., Meihua, J. T., Fakurazi, S., and Ithnin, H. (2013). The evolutionary development in drug discovery and delivery. **Journal of Drug Delivery Science and Technology.** 23(3): 195–205.
- Ishisaka, A., Ichikawa, S., Sakakibara, H., Piskula, M. K., Nakamura, T., Kato, Y., and Terao, J. (2011). Accumulation of orally administered quercetin in brain tissue and its antioxidative effects in rats. **Free Radical Biology and Medicine.** 51(7): 1329–1336.
- Itoigawa, M., Ito, C., Ju-ichi, M., Nobukuni, T., Ichiishi, E., Tokuda, H., and Furukawa, H. (2002). Cancer chemopreventive activity of flavanones on Epstein-Barr virus

- activation and two-stage mouse skin carcinogenesis. **Cancer Letters**. 176(1): 25–29.
- Jawahar, N., Meyyanathan, S. N., Reddy, G., and Sood, S. (2012). Solid lipid nanoparticles for oral delivery of poorly soluble drugs. **Journal of Pharmaceutical Science and Research**. 4(7): 1848–1855.
- Joycharat, N., Boonma, C., Thammavong, S., Yingyongnarongkul, B., Limsuwan, S., and Voravuthikunchai, S. P. (2016). Chemical constituents and biological activities of *Albizia myriophylla* wood. **Pharmaceutical Biology**. 54(1): 62–73.
- Joycharat, N., Thammavong, S., Limsuwan, S., Homlaead, S., Voravuthikunchai, S. P., Yingyongnarongkul, B., and Subhadhirasakul, S. (2013). Antibacterial substances from *Albizia myriophylla* wood against cariogenic *Streptococcus mutans*. **Archives of Pharmacal Research**. 36(6): 723–730.
- Khalil, R. M., El-bary, A. A., Kassem, M. A., Ghorab, M. M., and Ahmed, M. B. (2013). Solid lipid nanoparticles for topical delivery of meloxicam: development and *in vitro* characterization. **European Scientific Journal**. 4(7): 24–26.
- Khan, M. T. H., Orhan, I., Şenol, F. S., Kartal, M., Şener, B., Dvorská, M., and Šlapetová, T. (2009). Cholinesterase inhibitory activities of some flavonoid derivatives and chosen xanthone and their molecular docking studies. **Chemico-Biological Interactions**. 181(3): 383–389.
- Khan, S., Baboota, S., Ali, J., Khan, S., Narang, R., and Narang, J. (2015). Nanostructured lipid carriers: An emerging platform for improving oral bioavailability of lipophilic drugs. **International Journal of Pharmaceutical Investigation**. 5(4): 182.
- Khatun, Z., Nurunnabi, M., Cho, K. J., Byun, Y., Bae, Y. H., and Lee, Y. (2014). Oral

- absorption mechanism and anti-angiogenesis effect of taurocholic acid-linked heparin-docetaxel conjugates. **Journal of Controlled Release**. 177: 64–73.
- Kumavat, S. D., Chaudhari, Y. S., Borole, P., Mishra, P., Shenghani, K., and Duvvuri, P. (2013). Degradation studies of curcumin. **International Journal of Pharmacy Review and Research**. 3(2): 50–55.
- Kurien, B. T., and Scofield, R. H. (2007). Curcumin/turmeric solubilized in sodium hydroxide inhibits HNE protein modification—an *in vitro* study. **Journal of Ethnopharmacology**. 110(2): 368–373.
- Li, D.-C., Zhong, X.-K., Zeng, Z.-P., Jiang, J.-G., Li, L., Zhao, M.-M., and Gao, Y.-X. (2009). Application of targeted drug delivery system in Chinese medicine. **Journal of Controlled Release**. 138(2): 103–12.
- Liu, L., Guo, L., Zhao, C., Wu, X., Wang, R., and Liu, C. (2015). Characterization of the intestinal absorption of seven flavonoids from the flowers of *Trollius chinensis* using the Caco-2 cell monolayer model. **PLoS ONE**. 10(3): e0119263.
- Liu, Y., and Feng, N. (2015). Nanocarriers for the delivery of active ingredients and fractions extracted from natural products used in traditional Chinese medicine (TCM). **Advances in Colloid and Interface Science**. 221: 60–76.
- Lohr, J. W., Willsky, G. R., and Acara, M. A. (1998). Renal drug metabolism. **Pharmacological Reviews**. 50(1): 107-142.
- Lozoya-Agullo, I., Araújo, F., González-Álvarez, I., Merino-Sanjuán, M., González-Álvarez, M., Bermejo, M., and Sarmiento, B. (2017). Usefulness of Caco-2/HT29-MTX and Caco-2/HT29-MTX/Raji B coculture models to predict intestinal and colonic permeability compared to Caco-2 monoculture. **Molecular Pharmaceutics**. 14(4): 1264–1270.

- Mahidol, C., Prawat, H., Prachyawarakorn, V., and Ruchirawat, S. (2011). Investigation of some bioactive Thai medicinal plants. **Phytochemistry Reviews**. 1(3): 287–297.
- Mahidol, C., Prawat, H., Ruchirawat, S., Lihkitwitayawuid, K., Lin, L., and Coriell, G. A. (1997). Prenylated flavanones from *Derris reticulata*. **Phytochemistry**. 45(4): 7–11.
- Mahidol, C., Ruchirawat, S., Prawat, H., Pisutjaroenpong, S., Engprasert, S., Chumsri, P., and Picha, P. (1998). Biodiversity and natural product drug discovery. **Pure and Applied Chemistry**. 70(11): 2065–2072.
- Mancuso, C., Siciliano, R., Barone, E., and Preziosi, P. (2012). Natural substances and Alzheimer's disease: from preclinical studies to evidence based medicine. **Biochimica et Biophysica Acta - Molecular Basis of Disease**. 1822(5): 616–624.
- McKay, T. B., and Karamichos, D. (2017). Quercetin and the ocular surface: What we know and where we are going. **Experimental Biology and Medicine**. 242(6): 565–572.
- Md, S., Bhattmisra, S. K., Zeeshan, F., Shahzad, N., Mujtaba, M. A., Srikanth Meka, V., and Ali, J. (2018). Nano-carrier enabled drug delivery systems for nose to brain targeting for the treatment of neurodegenerative disorders. **Journal of Drug Delivery Science and Technology**. 43(October): 295–310.
- Mead, J., Irvine, S., and Ramji, D. (2002). Lipoprotein lipase: structure, function, regulation, and role in disease. **Journal of Molecular Medicine**. 80(12): 753–769.
- Mirvish, S. S. (1964). Bile acids and other lipids in the gall-bladder biles of africans with primary cancer of the liver. **British Journal of Cancer**. 18(3): 478–483.
- Monache, G. D., De Rosa, M. C., Scurria, R., Vitali, A., Cuteri, A., Monacelli, B., and

- Botta, B. (1995). Comparison between metabolite productions in cell culture and in whole plant of *Maclura pomifera*. **Phytochemistry**. 39(3): 575–580.
- Moorthi, C., and Kathiresan, K. (2013). Curcumin-piperine/curcumin-quercetin/curcumin-silibinin dual drug-loaded nanoparticulate combination therapy: a novel approach to target and treat multidrug-resistant cancers. **Journal of Medical Hypotheses and Ideas**. 7(1): 15–20.
- Mukherjee, S., Ray, S., and Thakur, R. S. (2009). Solid lipid nanoparticles: a modern formulation approach in drug delivery system. **Indian Journal of Pharmaceutical Sciences**. 71(4): 349–358.
- Mukhopadhyay, P., and Prajapati, A. K. (2015). Quercetin in anti-diabetic research and strategies for improved quercetin bioavailability using polymer-based carriers—a review. **RSC Advances**. 5(118): 97547–97562.
- Müller, H., and Eckhardt, C. J. (1978). Stress induced change of electronic structure in a polydiacetylene crystal. **Molecular Crystals and Liquid Crystals**. 45(3–4): 313–318.
- Muzzarelli, R. A. A. (2011). Chitosan composites with inorganics, morphogenetic proteins and stem cells, for bone regeneration. **Carbohydrate Polymers**. 83(4): 1433–1445.
- Nothnagel, L., and Wacker, M. G. (2018). How to measure release from nanosized carriers. **European Journal of Pharmaceutical Sciences**. 120: 199–211.
- O'Brien, R. W., Midmore, B. R., Lamb, A., and Hunter, R. J. (1990). Electroacoustic studies of moderately concentrated colloidal suspensions. **Faraday Discussions of the Chemical Society**. 90: 301–312.
- Oehlke, K., Behsnilian, D., Mayer-Miebach, E., Weidler, P. G., and Greiner, R. (2017).

- Edible solid lipid nanoparticles (SLN) as carrier system for antioxidants of different lipophilicity. **PLoS ONE**. 12(2): 1–18.
- Otsubo, Y. (2015). Use of Pharmacogenomics and biomarkers in the development of new drugs for Alzheimer disease in Japan. **Clinical Therapeutics**. 37(8): 1627–1631.
- Ou-Yang, Z., Cao, X., Wei, Y., Zhang, W. W. Q., Zhao, M., and Duan, J. ao. (2013). Pharmacokinetic study of rutin and quercetin in rats after oral administration of total flavones of mulberry leaf extract. **Brazilian Journal of Pharmacognosy**. 23(5): 776–782.
- Pacheco-Torres, J., Mukherjee, N., Walko, M., López-Larrubia, P., Ballesteros, P., Cerdan, S., and Kocer, A. (2015). Image guided drug release from pH-sensitive Ion channel-functionalized stealth liposomes into an in vivo glioblastoma model. **Nanomedicine: Nanotechnology, Biology and Medicine**. 11(6): 1345–1354.
- Park, K., Ki Lee, S., Hyun Son, D., Ah Park, S., Kim, K., Won Chang, H., and Kim, S. Y. (2007). The attenuation of experimental lung metastasis by a bile acid acylated-heparin derivative. **Biomaterials**. 28(16): 2667–2676.
- Park, K., Lee, G. Y., Kim, Y.-S., Yu, M., Park, R.-W., Kim, I.-S., and Byun, Y. (2006). Heparin–deoxycholic acid chemical conjugate as an anticancer drug carrier and its antitumor activity. **Journal of Controlled Release**. 114(3): 300–306.
- Picariello, G., Iacomino, G., Mamone, G., Ferranti, P., Fierro, O., Gianfrani, C., and Addeo, F. (2013). Transport across Caco-2 monolayers of peptides arising from *in vitro* digestion of bovine milk proteins. **Food Chemistry**. 139(1–4): 203–212.
- Pool, H., Mendoza, S., Xiao, H., and McClements, D. J. (2013). Encapsulation and release of hydrophobic bioactive components in nanoemulsion-based delivery

- systems: impact of physical form on quercetin bioaccessibility. **Food and Function**. 4(1): 162–174.
- Prasad, S. K., Laloo, D., Kumar, M., and Hemalatha, S. (2013). Antidiarrhoeal evaluation of root extract, its bioactive fraction, and lupinifolin isolated from *Eriosema chinense*. **Planta Medica**. 79(17): 1620–1627.
- Prawat, H., Mahidol, C., and Ruchirawat, S. (2000). Reinvestigation of *Derris reticulata*. **Pharmaceutical Biology**. 38(s1): 63–67.
- Priprem, A., Watanatorn, J., Sutthiparinyanont, S., Phachonpai, W., and Muchimapura, S. (2008). Anxiety and cognitive effects of quercetin liposomes in rats. **Nanomedicine: Nanotechnology, Biology, and Medicine**. 4(1): 70–78.
- Roche, H. M., Terres, A. M., Black, I. B., Gibney, M. J., and Kelleher, D. (2001). Fatty acids and epithelial permeability: effect of conjugated linoleic acid in Caco-2 cells. **Gut**. 48(6): 797–802.
- Rostami, E., Kashanian, S., Azandaryani, A. H., Faramarzi, H., Dolatabadi, J. E. N., and Omidfar, K. (2014). Drug targeting using solid lipid nanoparticles. **Chemistry and Physics of Lipids**. 181(April): 56–61.
- Sabogal-Guáqueta, A. M., Muñoz-Manco, J. I., Ramírez-Pineda, J. R., Lamprea-Rodríguez, M., Osorio, E., and Cardona-Gómez, G. P. (2015). The flavonoid quercetin ameliorates Alzheimer's disease pathology and protects cognitive and emotional function in aged triple transgenic Alzheimer's disease model mice. **Neuropharmacology**. 93(August): 134–145.
- Sáenz, J. M., and Asua, J. M. (1995). Dispersion polymerization in polar solvents. **Journal of Polymer Science Part A: Polymer Chemistry**. 33(9): 1511–1521.
- Salminen, H., Helgason, T., Aulbach, S., Kristinsson, B., Kristbergsson, K., and Weiss,

- J. (2014). Influence of co-surfactants on crystallization and stability of solid lipid nanoparticles. **Journal of Colloid and Interface Science**. 426: 256–263.
- Schneider, C., Gordon, O. N., Edwards, R. L., and Luis, P. B. (2015). Degradation of curcumin: from mechanism to biological implications. **Journal of Agricultural and Food Chemistry**. 63(35): 7606–7614.
- Shen, J., and Burgess, D. J. (2015). *In vitro-in vivo* correlation for complex non-oral drug products: Where do we stand? **Journal of Controlled Release**. 219: 644–651.
- Silva, J. C. da, Borrin, T. R., Ruy, P., Brito, T. C., Pinheiro, A. C., Vicente, A. A., and Pinho, S. C. (2014). Characterization, physicochemical stability, and evaluation of *in vitro* digestibility of solid lipid microparticles produced with palm kernel oil and tristearin. **Food Science and Technology**. 34(3): 532–538.
- Soonthornchareonnon, N., Ubonopas, L., Kaewsuwan, S., and Wuttiudomlert, M. (2004). Lupinifolin, a bioactive flavanone from *Myriopteron extensum* (Wight) K. Schum. stem. **Thai Journal of Phytopharmacy**. 11(2): 19–28.
- Souza, S. D. (2014). A review of *in vitro* drug release test methods for nano-sized dosage forms. **Advances in Pharmaceutics**. 2014(304757): 1–12.
- Sriraksa, N., Wattanathorn, J., Muchimapura, S., Tiamkao, S., Brown, K., and Chaisiwamongkol, K. (2012). Cognitive-enhancing effect of quercetin in a rat model of Parkinson's disease induced by 6-hydroxydopamine. **Evidence-Based Complementary and Alternative Medicine**. 2012: 823206.
- Suhailah, S. N. A. E., and Arabia, S. (2014). Quercetin nanoparticles: preparation and characterization. **Indian Journal of Drugs**. 2(3): 96–103.
- Sun, D., Li, N., Zhang, W., Yang, E., Mou, Z., Zhao, Z., and Wang, W. (2016).

- Quercetin-loaded PLGA nanoparticles: a highly effective antibacterial agent *in vitro* and anti-infection application *in vivo*. **Journal of Nanoparticle Research**. 18(1): 3–10.
- Sutthivaiyakit, S., Thongnak, O., Lhinhatrakool, T., Yodchun, O., Srimark, R., Dowtaisong, P., and Chuankamnerdkarn, M. (2009). Cytotoxic and antimycobacterial prenylated flavonoids from the roots of *Eriosema chinense*. **Journal of Natural Products**. 72: 1092–1096.
- Tan, B. J., Liu, Y., Chang, K. L., Lim, B. K. W., and Chiu, G. N. C. (2012). Perorally active nanomicellar formulation of quercetin in the treatment of lung cancer. **International Journal of Nanomedicine**. 7(February): 651–661.
- Thammavong, S. (2013). **Chemical constituents of *Albizia myriophylla* wood and biological activities**. (Master thesis, Prince of Songkla University, Songkla, Thailand). Retrieved from PSU Knowledge Bank.
- Thongnest, S., Lhinhatrakool, T., Wetprasit, N., Sutthivaiyakit, P., and Sutthivaiyakit, S. (2013). *Eriosema chinense*: a rich source of antimicrobial and antioxidant flavonoids. **Phytochemistry**. 96: 353–359.
- Tian, C., Asghar, S., Wu, Y., Chen, Z., Jin, X., Yin, L., and Xiao, Y. (2017). Improving intestinal absorption and oral bioavailability of curcumin via taurocholic acid-modified nanostructured lipid carriers. **International Journal of Nanomedicine**. 12: 7897–7911.
- Van Giau, V., and An, S. S. A. (2016). Emergence of exosomal miRNAs as a diagnostic biomarker for Alzheimer's disease. **Journal of the Neurological Sciences**. 360: 141–152.
- Wallace, S. J., Li, J., Nation, R. L., and Boyd, B. J. (2013). Encapsulation and release

- methodology. **Drug Delivery Translational Research**. 2(4): 284–292.
- Yang, L.-L., Xiao, N., Li, X.-W., Fan, Y., Alolga, R. N., Sun, X.-Y., and Qi, L.-W. (2016). Pharmacokinetic comparison between quercetin and quercetin 3-O- β -glucuronide in rats by UHPLC-MS/MS. **Nature**. 6(35460): 1–9.
- Yen, C., Chen, Y., Wu, M., Wang, C., and Wu, Y. (2018). Nanoemulsion as a strategy for improving the oral bioavailability and anti-inflammatory activity of andrographolide. **International Journal of Nanomedicine**. 13: 669–680.
- Yostawonkul, J., Surassmo, S., Namdee, K., Khongkow, M., Boonthum, C., Pagsesing, S., and Yata, T. (2017). Nanocarrier-mediated delivery of α -mangostin for non-surgical castration of male animals. **Scientific Reports**. 7(1): 16234.
- Yücel, Ç., and De, Z. (2016). Original article Development of cisplatin-loaded liposome and evaluation of transport properties through Caco-2 cell line. **Journal of Pharmaceutical Sciences**. 13(1): 69–80.
- Yue, P.-F., Lu, X.-Y., Zhang, Z.-Z., Yuan, H.-L., Zhu, W.-F., Zheng, Q., and Yang, M. (2009). The study on the entrapment efficiency and *in vitro* release of puerarin submicron emulsion. **Journal of the American Association of Pharmaceutical Scientists**. 10(2): 376–383.
- Yusook, K., Weeranantanapan, O., Hua, Y., Kumkrai, P., and Chudapongse, N. (2017). Lupinifolin from *Derris reticulata* possesses bactericidal activity on *Staphylococcus aureus* by disrupting bacterial cell membrane. **Journal of Natural Medicines**. 71(2): 357–366.
- Zhang, J., Tang, Q., Xu, X., and Li, N. (2013). Development and evaluation of a novel phytosome-loaded chitosan microsphere system for curcumin delivery.

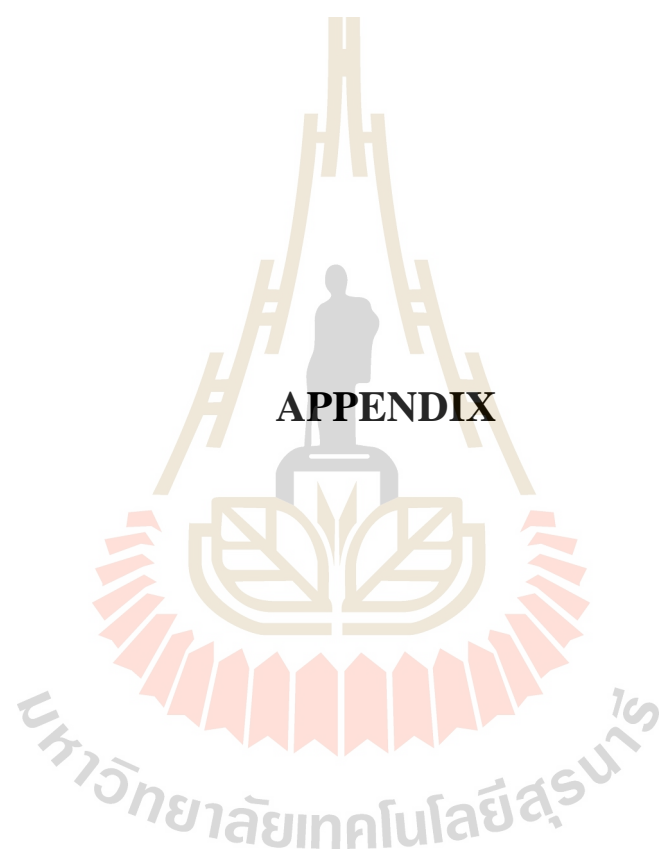
International Journal of Pharmaceutics. 448(1): 168–174.

Zhang, L. J., Liaw, C. C., Hsiao, P. C., Huang, H. C., Lin, M. J., Lin, Z. H., and Kuo, Y. H. (2014). Cucurbitane-type glycosides from the fruits of *Momordica charantia* and their hypoglycaemic and cytotoxic activities. **Journal of Functional Foods.** 6(1): 564–574.

Zhang, P., Chen, L., Gu, W., Xu, Z., Gao, Y., and Li, Y. (2007). *In vitro* and *in vivo* evaluation of donepezil-sustained release microparticles for the treatment of Alzheimer's disease. **Biomaterials.** 28(10): 1882–1888.

Zhang, X., Hu, J., Zhong, L., Wang, N., Yang, L., Liu, C. C., and Zhuang, J. (2016). Quercetin stabilizes apolipoprotein E and reduces brain A β levels in amyloid model mice. **Neuropharmacology.** 108: 179–192.

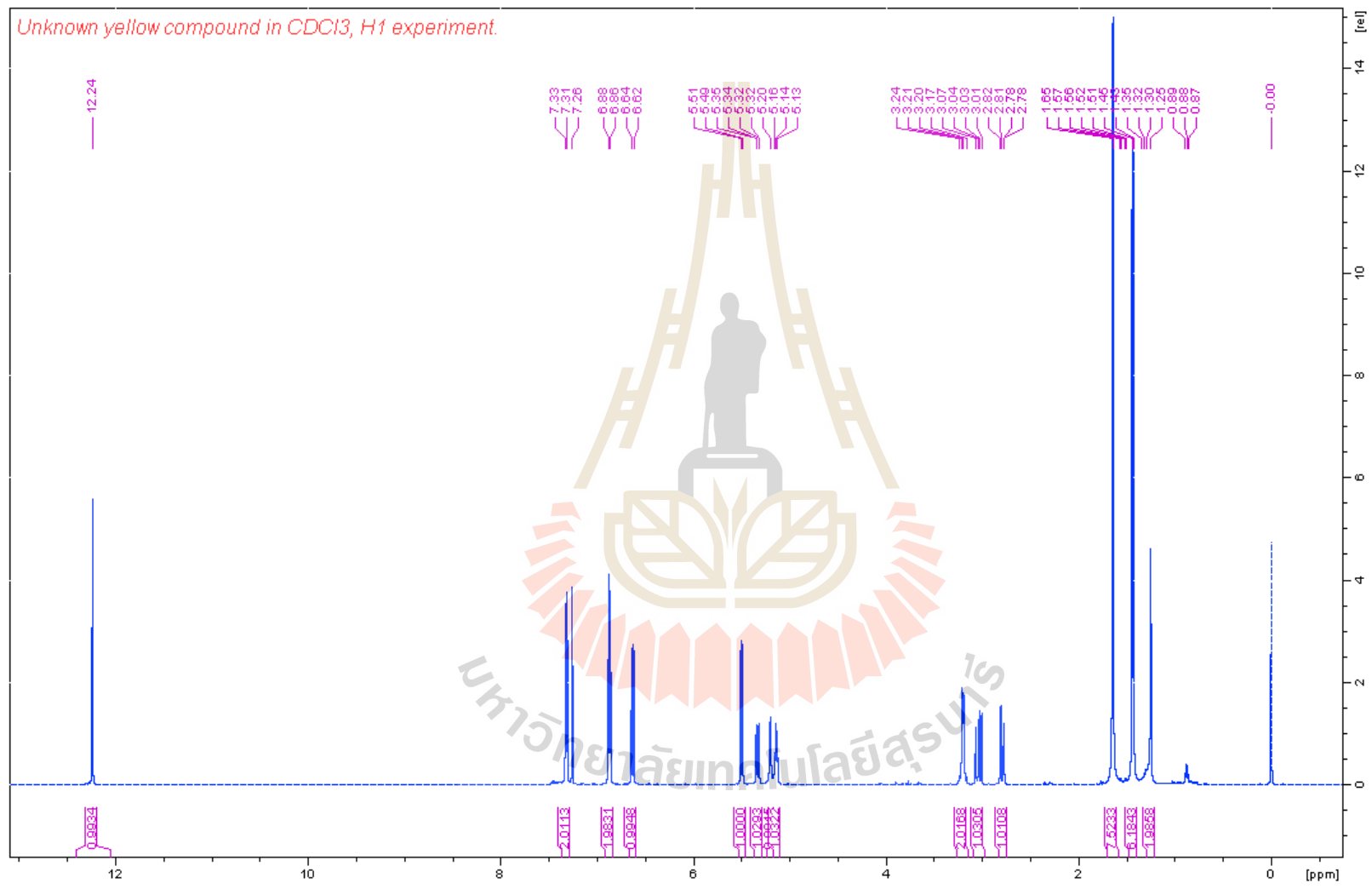
Zhao, B. (2009). Natural antioxidants protect neurons in Alzheimer's disease and Parkinson's disease. **Neurochemical Research.** 34(4): 630–638.



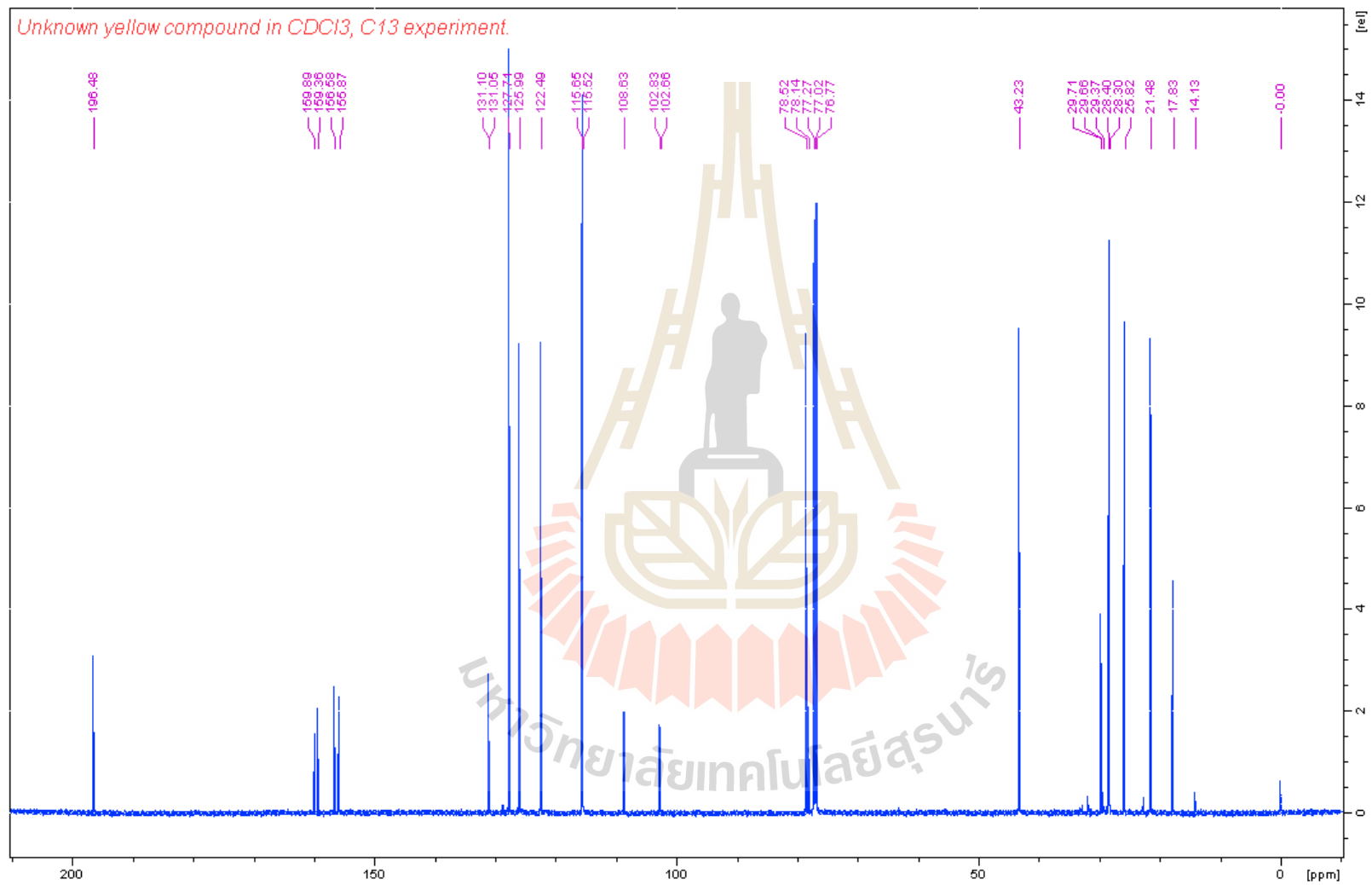
APPENDIX

APPENDIX
NMR SPECTROSCOPY





¹H - Nuclear magnetic resonance (NMR) spectroscopy of yellow crystals from *A. myriophylla*



¹³C - Nuclear magnetic resonance (NMR) spectroscopy of yellow crystals from *A. myriophylla*

CURRICULUM VITAE

Name: Miss Jidapa Musika

Date of birth: March 4, 1988

Place of birth: Trang, Thailand

Education: B.Sc. (Computational Science, First class honors, gold medal), 2009,
Walailak University

M.Sc. (Ecology and Biodiversity), 2014, Walailak University

Publication:

Musika, J., Khongchatee, A., and Phinchongsakuldit, J. (2014). Reanalysis and revision of the complete mitochondrial genome of *Rachycentron canadum* (Teleostei, Perciformes, Rachycentridae). *Mitochondrial DNA*, 25(4), 249–250.

Musika, J., and Phinchongsakuldit, J. (2013). Live sharksucker *Echeneis naucrates* (Linnaeus 1758) mitochondrial genome: the first report of Echeneidae complete mitochondrial genome. *Mitochondrial DNA*, 1736, 1–2.

Grant: Science Achievement Scholarship of Thailand (2011-2017)

Position and workplace: -